

This article appeared in a journal published by Elsevier. The attached copy is furnished to the author for internal non-commercial research and education use, including for instruction at the authors institution and sharing with colleagues.

Other uses, including reproduction and distribution, or selling or licensing copies, or posting to personal, institutional or third party websites are prohibited.

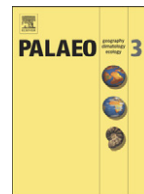
In most cases authors are permitted to post their version of the article (e.g. in Word or Tex form) to their personal website or institutional repository. Authors requiring further information regarding Elsevier's archiving and manuscript policies are encouraged to visit:

<http://www.elsevier.com/copyright>



Contents lists available at ScienceDirect

Palaeogeography, Palaeoclimatology, Palaeoecology

journal homepage: www.elsevier.com/locate/palaeo

The Mendel Formation: Evidence for Late Miocene climatic cyclicity at the northern tip of the Antarctic Peninsula

Daniel Nývlt^{a,*}, Jan Košler^{b,c}, Bedřich Mlčoch^b, Petr Mixa^b, Lenka Lisá^d,
Miroslav Bubík^a, Bart W.H. Hendriks^e

^a Czech Geological Survey, Brno branch, Leitnerova 22, 658 69 Brno, Czechia

^b Czech Geological Survey, Klárov 3, 118 21 Praha 1, Czechia

^c Department of Earth Science, University of Bergen, Allegaten 41, Bergen, Norway

^d Institute of Geology of the Czech Academy of Sciences, v.v.i., Rozvojová 269, 165 02 Praha, Czechia

^e Geological Survey of Norway, Leiv Eirikssons vei 39, 7491 Trondheim, Norway

ARTICLE INFO

Article history:

Received 31 May 2010

Received in revised form 9 November 2010

Accepted 13 November 2010

Available online 19 November 2010

Keywords:

Antarctic Peninsula

James Ross Island

Miocene

Climatic cyclicity

Diamictites

Quartz microtextures

Micropaleontology

⁸⁷Sr/⁸⁶Sr dating

⁴⁰Ar/³⁹Ar dating

James Ross Island Volcanic Group

Paleoenvironment

ABSTRACT

A detailed description of the newly defined Mendel Formation is presented. This Late Miocene (5.9–5.4 Ma) sedimentary sequence with an overall thickness of more than 80 m comprises cyclic deposition in terrestrial glacial, glaciomarine and marine environments. Subglacial till was deposited by a thick grounded Antarctic Peninsula ice stream advancing eastwards through the Prince Gustav Channel, crossing the northernmost part of present-day James Ross Island, with most of the material carried actively at the base of the warm-based glacier. The form of the Prince Gustav Channel originated before the late Miocene and its present glacial over-deepening resulted in multiple grounded glacier advances during the Neogene and Quaternary. The sea prograded from the east and the glacier margin became buoyant, building a small ice shelf, below and in front of which glaciomarine and marine sediments were deposited. These sedimentary deposits are composed of material that was transported mostly by small glaciers and subsequently by the floating ice shelf and by calving icebergs towards the open sea. These environmental and glaciological conditions differ strongly from the present cold-based local glaciers of James Ross Island and the Antarctic Peninsula. These changes were triggered by the global sea level fluctuation connected with climatic changes due to Antarctic ice sheet build up and decay. This reveals Late Miocene obliquity-driven cyclicity with a ~41 ka period. The Mendel Formation sedimentary sequence is comprised of at least two glacial periods and one interglacial period. Sea level rise at the northern tip of the Antarctic Peninsula between glacial lowstand and interglacial highstand was more than 50 m during the late Miocene and was followed by a subsequent sea level fall of at least the same magnitude. The presence of well-preserved, articulated pectinid bivalves support “interglacial” open sea conditions. The re-deposition of palaeontological material was shown to be important for the Mendel Formation. Reworked pectinid shells revealed an open marine “interglacial” condition in this part of the Antarctic Peninsula during the Early to Mid Miocene (20.5–17.5 Ma). Unfortunately, relevant sedimentary deposits have not been found on land.

© 2010 Elsevier B.V. All rights reserved.

1. Introduction

Neogene glacial and glaciomarine deposits have been found in several places in Antarctica during the last few decades. Different glacial lithostratigraphic units are known from East Antarctica, including the Sirius Group in the Transantarctic Mts. (e.g. Hambrey et al., 2003; Stroeven, 1997; Webb et al., 1996; Wilson et al., 1998), the Sørsdal Formation in Vestfold Hills (e.g. Harwood et al., 2000; Quilty et al., 2000), Pliocene sedimentary deposits in Heidemann Valley (Colhoun et al., 2010), the Pagodroma Formation in the Prince

Charles Mts. (e.g. Hambrey and McKelvey, 2000; McKelvey et al., 2001), the unnamed glacial succession in the Grove Mts. (Fang et al., 2005), and many others.

Initial Antarctic glaciation during the Oligocene was astronomically controlled (Pälike et al., 2006), and Oligocene glacial deposits in the West Antarctic are known from the northernmost part of the Antarctic Peninsula (AP). The oldest glacial sedimentary deposits are at the top of the La Meseta Formation on Seymour Island (Ivany et al., 2004, 2006) and are dated to the Oi-1 glaciation event (Pälike et al., 2006) – close to the Eocene/Oligocene transition (~34 Ma), however these results are disputed by others, as the dated palaeontological material may be reworked to much younger deposits (Gaždicki et al., 2004; Marenssi et al., 2010). Other Oligocene glacial sequences are known from King George Island as the Polonez Cove and Cape Melville

* Corresponding author. Tel.: +420 543429265; fax: +420 543212370.
E-mail address: daniel.nyvt@geology.cz (D. Nývlt).

Formations: ~30 Ma and ~23 Ma (Birkenmajer, 1982; Birkenmajer and Gaždicki, 1986; Birkenmajer et al., 1991; Dingle et al., 1997; Troedson and Smellie, 2002). They correlate with glacial events of the uppermost Oligocene witnessed by $\delta^{18}\text{O}$ values from carbonates in ODP leg 199 in the equatorial Pacific (Pälike et al., 2006). Several younger glacial/interglacial sedimentary sequences occur below and within the James Ross Island Volcanic Group (JRIVG) in the James Ross Basin, namely on Seymour Island (e.g. Doktor et al., 1988; Gaždicki et al., 2004; Malagnino et al., 1981; Zinsmeister and de Vries, 1983); Cockburn Island (e.g. Andersson, 1906; Gaždicki and Webb, 1996; Hennig, 1911; Jonkers, 1998a; McArthur et al., 2006; Williams et al., 2010); Vega Island (e.g. Hambrey and Smellie, 2006; Lirio et al., 2007; Pirrie et al., 1991; Smellie et al., 2006, 2008); Tail Island (Pirrie and Sykes, 1987); and on James Ross Island (Andersson, 1906; Bibby, 1966; Carrizo et al., 1998; Clark et al., 2010; Concheyro et al., 2005, 2007; del Valle et al., 1987; Dingle and Lavelle, 1998; Hambrey and Smellie, 2006; Hambrey et al., 2008; Jonkers et al., 2002; Lirio and del Valle, 1997; Lirio et al., 2003; Marenssi et al., 1987; Nelson, 1966; Nelson et al., 2009; Nordenskjöld, 1905; Pirrie et al., 1997; Smellie et al., 2006, 2008; Strelin et al., 1997).

The Cenozoic sedimentary successions around Antarctica allow the reconstruction of palaeoenvironmental and palaeogeographical conditions in the terrestrial and surrounding oceans. These reconstructions are crucial not only for understanding climatic changes connected with advances and retreats of the East and West Antarctic ice sheets, but they are also important for modelling future climatic change in the Antarctic.

This paper aims to be a detailed multidisciplinary study of an extensive and thick sedimentary deposit in the Ulu Peninsula, on the northernmost part of James Ross Island (JRI). The stratigraphical, sedimentological, palaeontological, and age dating results from this region allow reconstruction of the palaeoenvironment and palaeoclimate for this part of JRI in a short time interval in the latest Miocene.

2. Timing of glacial and glaciomarine sedimentary units associated with the James Ross Island Volcanic Group on James Ross Island

Sedimentary deposits found in association with volcanic rocks of the JRIVG on JRI fall into different age intervals of the Neogene and Quaternary. The age of these units was determined mostly by $^{87}\text{Sr}/^{86}\text{Sr}$ dating of pectinid bivalves and $^{40}\text{Ar}/^{39}\text{Ar}$ dating of associated volcanic rocks. The available $^{87}\text{Sr}/^{86}\text{Sr}$ ages are listed in Table 1. Numerous sedimentary successions are intercalated in the JRIVG; for the most

part, they do not contain fossils and may be dated only using underlying or overlying volcanic rocks. The most thorough list of available $^{40}\text{Ar}/^{39}\text{Ar}$ dates (69 age determinations) from JRI was recently presented by Smellie et al. (2008), who described at least 50 individual eruptive phases during the last 6.2 Ma. According to our field mapping in the northern Ulu Peninsula, JRI we know at present at least 70 localities with sedimentary sequences associated with the JRIVG, however most of them do not contain datable fossil material.

Some of the dates listed in Table 1 should be accepted with caution because the sedimentary environment of the deposits has not been studied in detail. A potential source of error in interpreting the $^{87}\text{Sr}/^{86}\text{Sr}$ dates lies in the reworking of shell fragments into the subglacial terrestrial or glaciomarine environment, as is common in many sedimentary units of the JRIVG. Strontium dating should therefore be supported by a detailed evaluation of the sedimentary environment and/or by $^{40}\text{Ar}/^{39}\text{Ar}$ dating of associated lavas. It will be demonstrated that shell reworking is an important factor in the interpretation of Sr isotopic ages in the Mendel Formation.

3. Field sites and methods

3.1. Sedimentary field and laboratory methods

The sites investigated in this study lie in the northernmost part of the Ulu Peninsula, between Cape Lachman, Berry Hill and the Czech Antarctic Johann Gregor Mendel Base (Fig. 1). Six sections of the 13 natural exposures (see Fig. 1 for localities), with individual thicknesses between 6 and 20 m, have been studied using standard sedimentological analyses, such as lithofacies logging, textural, fabric, palaeoflow and striation measurements. Sedimentary units were sampled for sedimentary petrological analyses, such as clast shape and roundness, surface features, and statistical and microscopic analyses. Visible macrofossils and samples for microfossil analyses have also been collected together with the underlying volcanic rocks.

Facies analyses have been undertaken using the lithofacies designations for glacial and poorly sorted sediments modified for Antarctic glacial and glaciomarine sediments by M. Hambrey (Benn and Evans, 1998; Hambrey, 1994; Hambrey and McKelvey, 2000; Moncrieff, 1989). Geographic north values of clast fabric and palaeoflow measurements were used throughout this study. Three dimensional clast fabric analyses were undertaken on terrestrial glacial units, measuring 25 elongated pebbles for each sample to distinguish individual subglacial till types (Benn, 1994; Lawson, 1979). The evaluation of clast shape is based on the Benn and Ballantyne (1993) modification of the Sneed and Folk (1958) equilateral ternary diagram and was undertaken on 25 basalt pebbles for each sample. All ternary diagrams were plotted using the spreadsheet program of Graham and Midgley (2000). The C_{40} index gives the percentage of clasts with a c:a ratio of <0.4 (Ballantyne, 1982). Clast roundness is based on the discrimination into the six main groups of Powers (1953). The RA index is defined as the percentage of very angular and angular clasts; the arbitrary threshold value for Krumbein's visual roundness of 0.25 has been adopted in this study. Overall clast form is expressed in covariant plots of the C_{40} index versus RA index (Benn and Ballantyne, 1994). Surface features (striae, facets, chatter marks or bullet-shapes) were also recorded. Macroscopic petrological analyses were undertaken for some units. Different petrologies have also been studied microscopically.

3.2. Quartz microtextures

The 0.25–0.5 mm fraction was separated for study of microtextures of quartz sand grains from diverse environments. The fraction was boiled for 20 min in 10% hydrochloric acid to remove calcium

Table 1
Summary of available $^{87}\text{Sr}/^{86}\text{Sr}$ dates from James Ross Island.

Locality	$^{87}\text{Sr}/^{86}\text{Sr}$	Mean Sr age (Ma)	Error (+/–)	Reference
Rabot Point	0.70893	9.9	0.97/0.97	Dingle and Lavelle (1998)
Fjordo Belén	(not given)	6.8	1.3/0.5	Jonkers (1998b)
Eastern Forster Cliffs	0.708971	6.45	0.31/0.21	Smellie et al. (2006)
Rockfall Valley – Stoneley Point	0.708977	6.31	0.32/0.14	Nelson et al. (2009)
Rhino Cliffs	0.709007	5.77	0.23/0.30	Nelson et al. (2009)
Jonkers Mesa – Pecten Spur	0.709022	5.44	0.20/0.27	Nelson et al. (2009)
Forster Cliffs	0.709034	5.06	0.35/0.41	Smellie et al. (2006)
Eastern Forster Cliffs	0.709038	4.93	0.35/0.51	Smellie et al. (2006)
Blancmange Hill	0.709039	4.89	0.35/0.53	Nelson et al. (2009)
Cape Gage	0.709043	4.74	0.32/0.63	Smellie et al. (2006)
Forster Cliffs	0.709051	4.23	0.51/0.95	Smellie et al. (2006)
SW Croft Bay	0.709069	2.54	0.86/0.36	Smellie et al. (2006)
Terrapin Hill	(Not given)	1.95	1.12/0.52	Lirio et al. (2003)

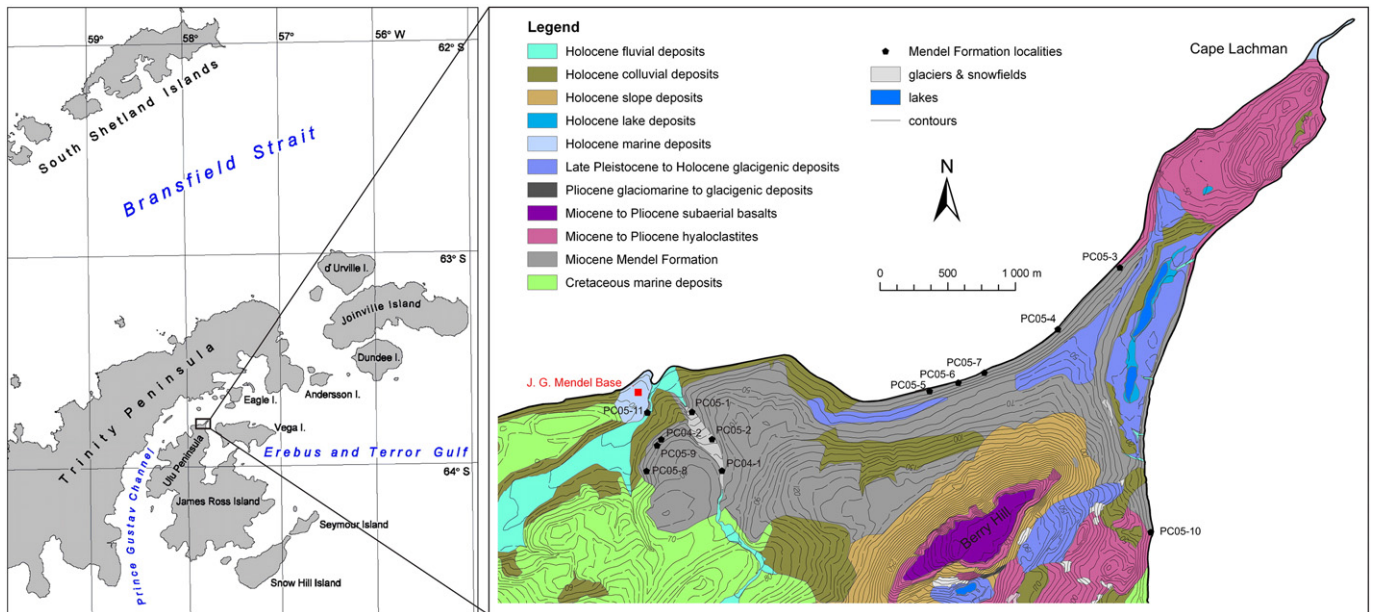


Fig. 1. Geological sketch map of the northernmost part of the Ulu Peninsula, James Ross Island with the extent of the Mendel Formation sedimentary deposits and studied sections shown. Topography based on the topographic map at 1:25,000 scale (Czech Geological Survey, 2009). Geology based on field mapping made by B. Mlčoch and D. Nývlt.

carbonate, iron staining and adhering particles, and then washed in distilled water. Dilute sodium hexametaphosphate (calgon solution) was then added for shaking. The suspension was then boiled in a stannous chloride solution to remove any iron oxide coatings. Approximately 30–50 grains were randomly picked, mounted on double sided graphite adhesive fixed to aluminium specimen stubs for SEM viewing and gold-coated. SEM photographs were made for further interpretations. All morphological, mechanical and chemical features were noted and described according to the propositions of Bull (1986), Helland et al. (1997) and Fuller and Murray (2002).

3.3. ⁴⁰Ar/³⁹Ar dating

Irradiation for argon dating was undertaken at the McMaster Nuclear Reactor Facility, Hamilton, Canada. The samples at McMaster were irradiated for 16 h 50 m (50 MWH) with a nominal neutron flux of $4 \cdot 10^{13} \text{ n cm}^{-2} \text{ s}^{-1}$. The nominal temperature of the irradiation site is <50 °C (M. Butler, pers. comm.). The production of isotopes of Ca

and K was determined by irradiation of CaF and K₂SO₄ salts, giving values of ^{36/37}Ca = 0.000298, ^{39/37}Ca = 0.000702 and ^{40/39}K = 0.0267, respectively. The samples were analysed at the ⁴⁰Ar/³⁹Ar Geochronology Laboratory at the Norwegian Geological Survey. Gas released during ablation was cleaned in the extraction line for 11 min using two pairs of SAES AP-10 getters, mounted in isolated sections of the line, each maintained with its own vacuum pump. The purified gas was then analysed in an MAP 215-50 mass spectrometer. The data for blanks, monitors and unknowns were collected on a Johnson electron multiplier with a gain setting of 1, while the magnet was automatically scanned over masses 35 through 41 in a cycled 'peak-hop' mode. Masses 37 through 40 were each measured in eight cycles and 10 counts per mass per cycle; mass 36 was measured with 20 counts per cycle. Sample data were corrected for blanks prior to being reduced with the IAAA (Interactive Ar–Ar Analysis) software package (Visual Basic programming for PC Windows) written by T.H. Torsvik and N.O. Arnaud and based in part on equations from Steiger and Jäger (1977), Dalrymple et al. (1981) and McDougall and Harrison (1999). Data

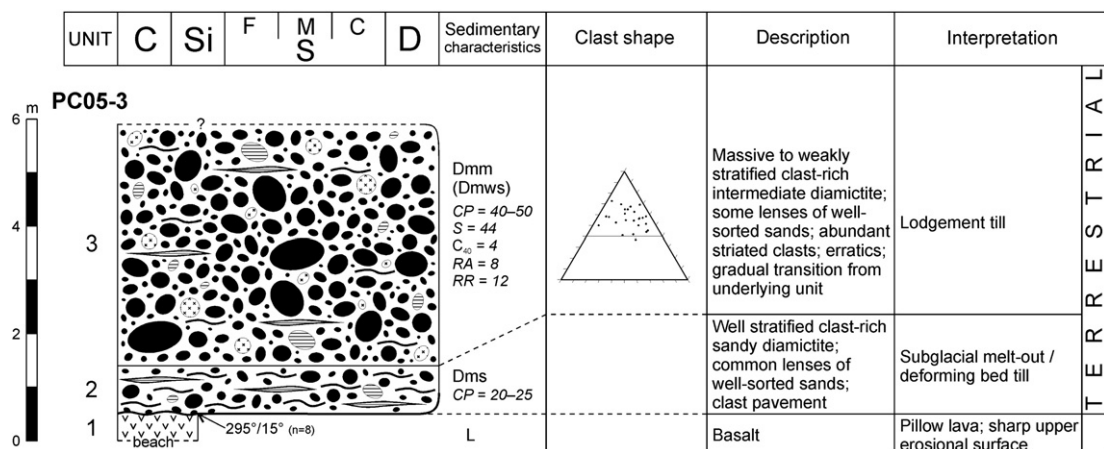


Fig. 2. Sedimentary log with description and interpretation of depositional environment at the PC05-3 section of the Mendel Formation with underlying lava flow at the neck of Cape Lachman. Facies codes according to Hambrey (1994) and Benn and Evans (1998), clast shape of basalts is given in the equilateral ternary diagram of Benn and Ballantyne (1993). CP is the percentage of gravel clasts; S is the percentage of striated clasts; C₄₀ is the percentage of clasts with c/a ratios of <0.4; RA is the percentage of very angular and angular clasts. Orientation data for erosional surfaces, lamination and cross bedding are also presented.

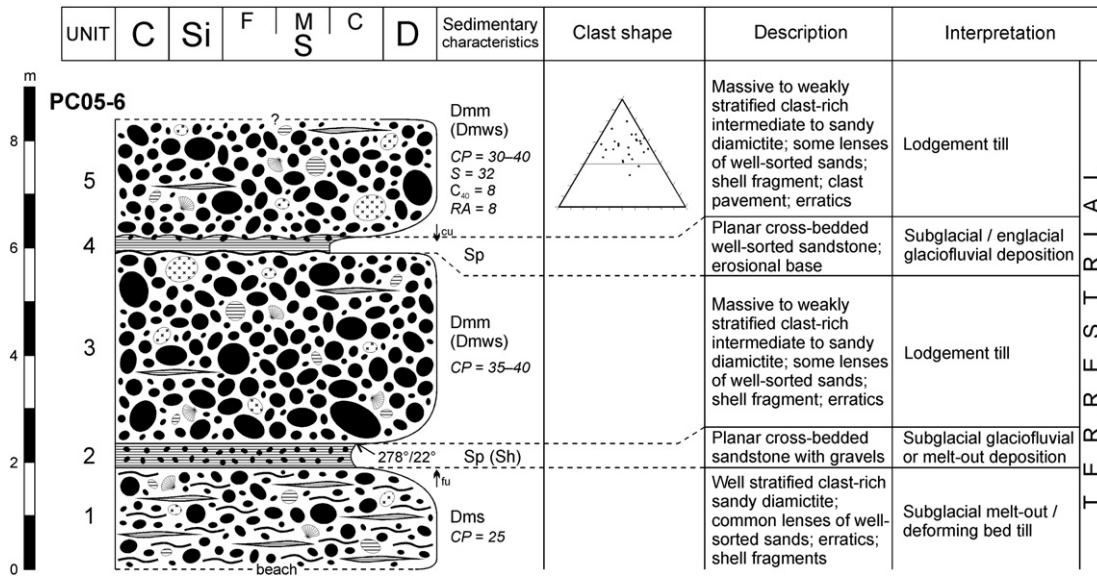


Fig. 3. Sedimentary log with description and interpretation of the depositional environment at the PC05-6 section of the Mendel Formation at the beach of the coast between the Mendel Base and Cape Lachman. For abbreviations and further explanation see Fig. 2.

reduction in IAAA incorporates corrections for interfering isotopes, mass discrimination (measured with an air pipette; 287.5), error in blanks and decay of ³⁷Ar.

3.4. ⁸⁷Sr/⁸⁶Sr dating

The pecten shells were repeatedly cleaned in an ultrasonic bath in DI water and visually checked under the microscope for potential surface contamination. The Sr isotopes in the pulverised shells (~100 mg) were measured in a Finnigan 262 mass-spectrometer at

the Department of Earth Science, University of Bergen. Chemical processing was carried out in a clean-room environment, using reagents purified in two-bottle Teflon stills. Samples were dissolved in 3 N HNO₃ and Sr was separated by specific extraction chromatography using an Eichron Sr-Spec resin. Sr samples were loaded on a double Re-filament and analysed in static mode. The ⁸⁷Sr/⁸⁶Sr isotopic ratios were corrected for mass fractionation using a ⁸⁸Sr/⁸⁶Sr ratio of 8.3752. Repeated measurements of the NBS-987 standard in the course of this study gave an average ⁸⁷Sr/⁸⁶Sr value of 0.710240 with an analytical uncertainty of ± 0.000019 (2 sigma). Ages derived from

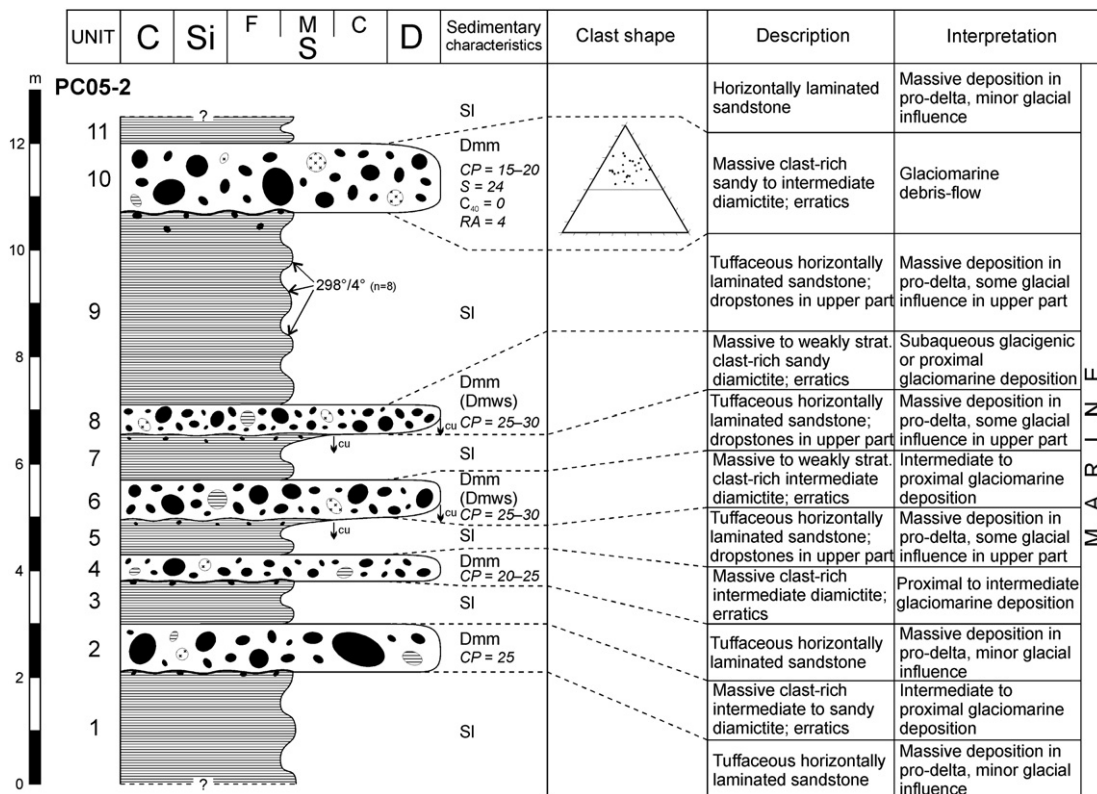


Fig. 4. Sedimentary log with description and interpretation of depositional environment at the PC05-2 section of the Mendel Formation close to Mendel Base. For abbreviations and further explanation see Fig. 2.

the isotopic composition of Sr in the pecten shells were calculated using the LOWESS 3:10 curve for Sr isotopic evolution in sea water (McArthur et al., 2001).

3.5. Micropalaeontology

Samples for micropalaeontology were processed by standard laboratory methods. More lithified samples were crushed using hydraulic press, soaked with a sodium bicarbonate solution, and finally washed on a 0.063 mm sieve. Microfossils were picked under a binocular microscope. The picked amount of residue exceeded 40 g per sample. All samples were extremely poor in microfossils and organic remnants.

4. Lithofacies description and interpretation

The interpretations are based on the lithofacies designation for Antarctic poorly sorted glacial sedimentary deposits (Benn and Evans, 1998; Hambrey, 1994; Hambrey and McKelvey, 2000), and six lithofacially different sediment types were defined. Lithofacies description is complemented by clast fabric, palaeoflow and striation measurements, microtextures of quartz sand grains and other sedimentary petrological methods (e.g. clast shape, roundness and surface features of gravels). Individual facies types present in the Mendel Formation are described below and in Figs. 2–7 and photographically illustrated in Fig. 8. The interpretation of the depositional environment is based on the lithofacies description and

the evaluation of the sedimentary petrological data. Overall micro-textural features are given in Fig. 9. SEM microphotographs of typical features are shown in Fig. 10. 3-D measurements of the fabric of clasts from terrestrial subglacial till units were plotted on contoured stereonet and a ternary diagram of their fabric shape using the method proposed by Benn (1994) is given in Fig. 11. A covariant plot of clast shape and roundness indices is given in Fig. 12.

4.1. Terrestrial sediments

4.1.1. Lodgement till

Lodgement till is the most common type of terrestrial sedimentary rocks found in the Mendel Formation; it was documented at the PC04-1, PC05-3, PC05-4, PC05-5, PC05-6, PC05-7 and PC05-8 sections. It is typically a massive or sometimes weakly stratified, matrix-supported, clast-rich, intermediate to sandy diamictite, occasionally with lenses of stratified sandy diamictites (Dmm, Dmws) and common striated clasts up to 1 m or more, and high amounts of erratic rocks (see Fig. 8B and D). The thickness of individual lodgement tills ranges from 3 to 7 m. They usually contain 30–50% of gravel clasts and 30–40% of them are striated (see Fig. 8E). Typically 90–95% of the gravel clasts are local (JRIVG) basalts, the rest is composed of local Cretaceous sandstone, siltstone or conglomerate and erratic phyllite, gneiss, or granitoid derived from the AP (see detailed petrographic descriptions of erratic rocks below). The relative volume of erratics varies between 1 and 5%. Most of the gravel clasts are subangular to subrounded (~80%); only ~12% of them are rounded. Basalt gravel clasts typically have

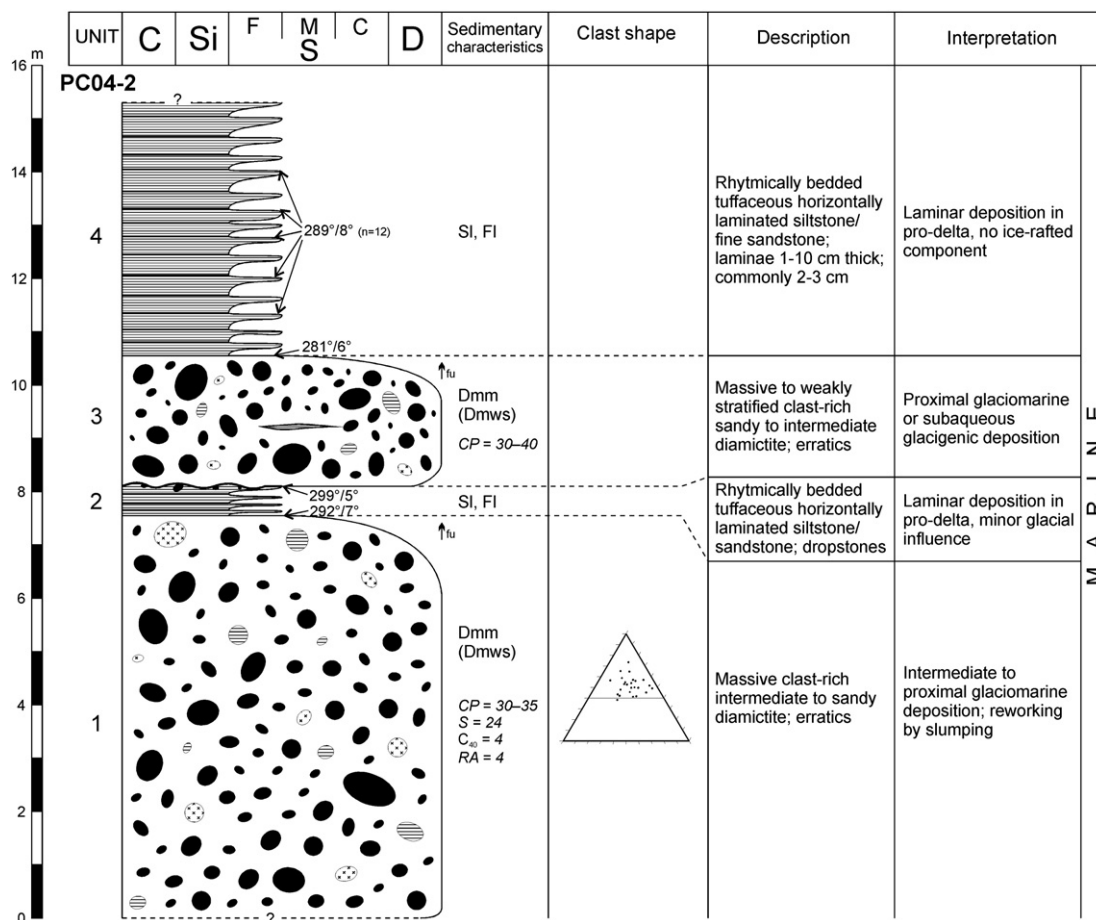


Fig. 5. Sedimentary log with description and interpretation of depositional environment at the PC04-2 section of the Mendel Formation close to Mendel Base. For abbreviations and further explanation see Fig. 2.

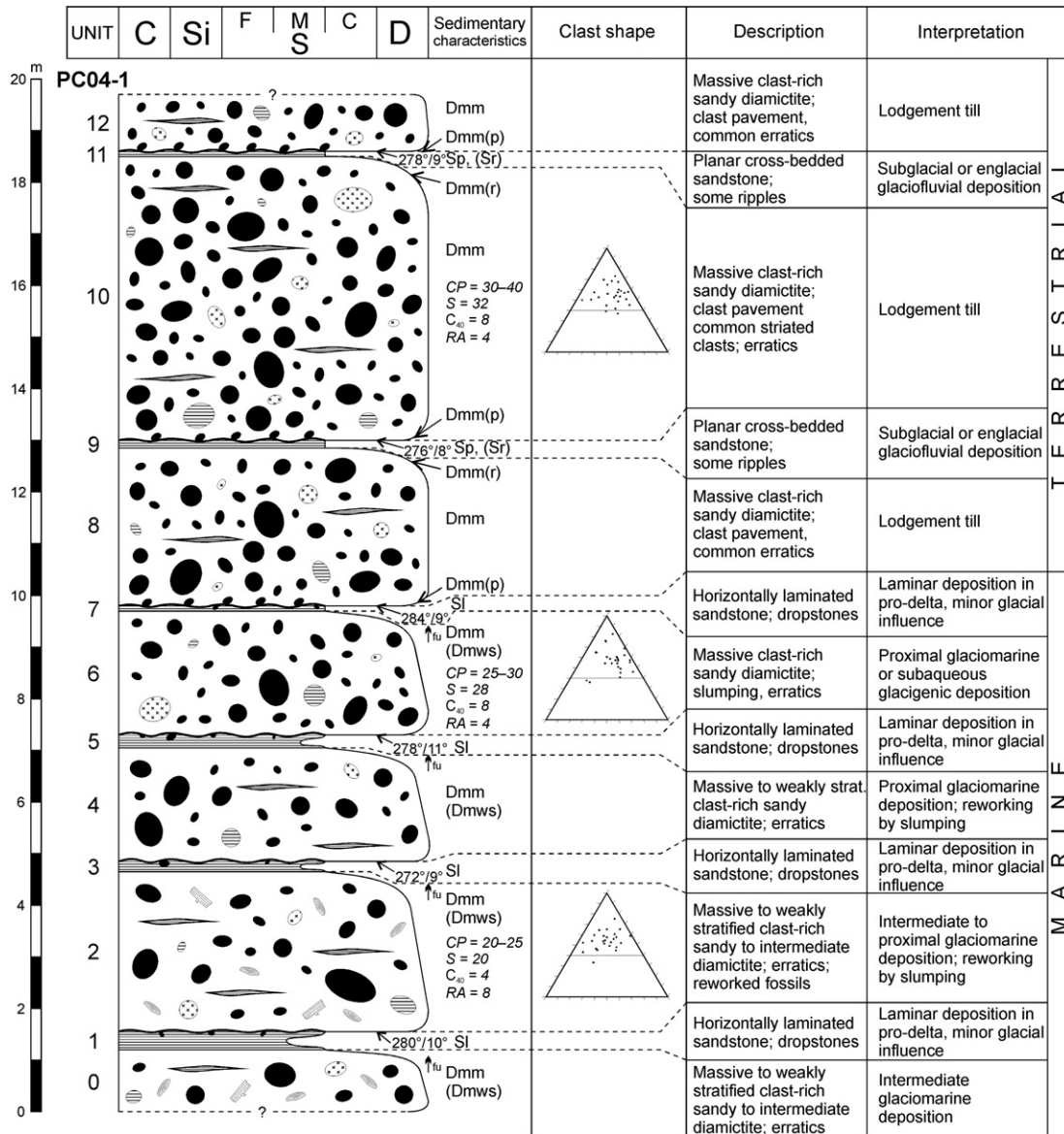


Fig. 6. Sedimentary log with description and interpretation of depositional environment at the PC04-1 section of the Mendel Formation close to Mendel Base. For abbreviations and further explanation see Fig. 2.

intermediate to high values of general sphericity (*c/a* values between 0.4 and 0.7) with slight rod affinity and *C*₄₀ indices of only 4–12% (see the individual lodgement tills in Figs. 2–7). The preferred orientation of the clast fabric is mostly medium, with *S*₁ eigenvalues being 0.55–0.58 indicating a girdle to cluster clast fabric (see Fig. 11). The main eigenvector (*V*₁) dips towards the W (275–295°), and the second most significant eigenvector (*V*₂) is perpendicular to the main one dipping towards the S (185–201°). Some lodgement tills (units PC05-6/5, PC05-8/1) contain reworked fragments of pectinid shells, which have been used for strontium dating (see the dating results below). Lodgement tills have mostly sharp erosional bases with clast pavements above fine-grained sediments, but they can also grade gradually from underlying melt-out tills and can also bear evidences of melt-out processes and lenses of stratified sands or sandy diamictites.

Quartz grains in the sand fraction are mainly subangular to subrounded (Fig. 10.1). Rounded and angular grains are less common or sometimes almost absent. The relief of the grains is predominantly medium; less common is high relief and the presence of low relief is limited. Mechanical features are represented mainly by edge abrasion

(Fig. 10.4), dish-shaped concavities (Fig. 10.1), straight steps and grooves (Fig. 10.4), large breakage (Fig. 10.4) and imbricated blocks (Fig. 10.1) or upturned or broken plates. Conchoidal fractures (Fig. 10.4) are less common and arcuate steps, striations, meandering ridges, V-shaped pits and curved grooves are absent or very rare. Chemical features are typical for medium to strong post-sedimentary weathering conditions. Extensive silica precipitation and grains with adhering particles (Fig. 10.2) are usually present. Solution pits and chemical V-shaped pits are rather rare or absent.

4.1.2. Subglacial melt-out till

A subglacial melt-out till was found to be the lowermost member of the Mendel Formation (unit PC05-3/2, PC05-4/2, PC05-6/1); it was also documented at the PC05-8 section. It is a well-stratified, matrix-supported, clast-rich, sandy diamictite (Dms), with ~20–25% gravel clasts and typical thicknesses of 1–3 m. Well-sorted sand lenses are common in subglacial melt-out tills. The lower boundary could be erosional (at the PC05-3 section above the pillow lava, see Fig. 8A), but sometimes also gradational, sometimes with striated clasts paved on the bottom surface due to the melt-out of finer particles from

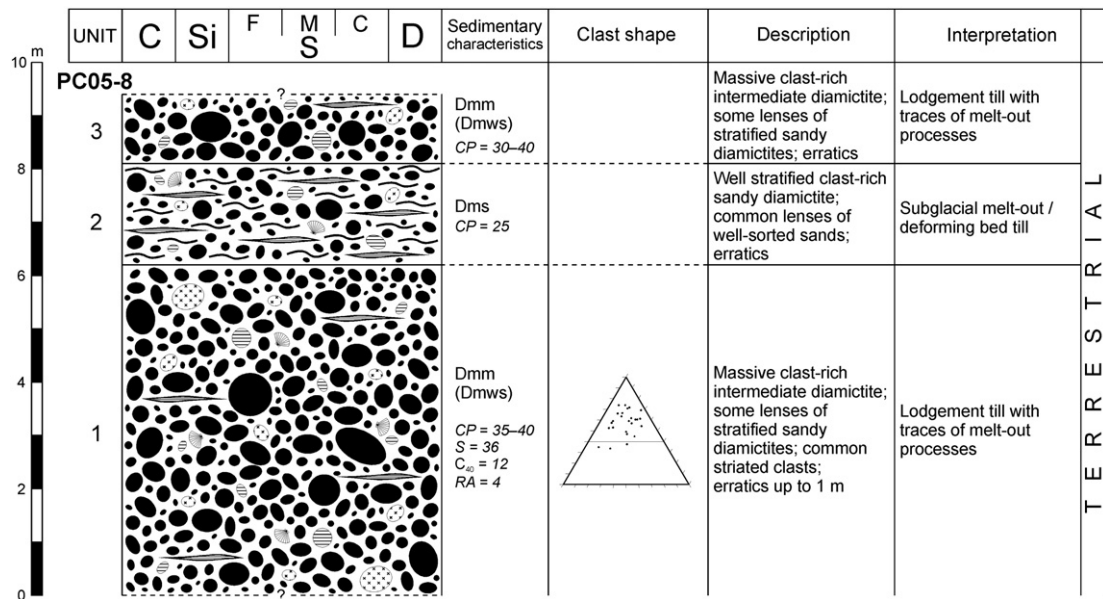


Fig. 7. Sedimentary log with description and interpretation of depositional environment at the PC05-8 section of the Mendel Formation close to Mendel Base. For abbreviations and further explanation see Fig. 2.

underlying units. The matrix of subglacial melt-out till is typically sandier and contains lower amounts of gravel clasts and less erratic rocks, than the overlying corresponding lodgement till. Flow structures are common as are lenses of well-sorted medium- to coarse-grained sands up to 10 cm thick, which can in certain places (unit PC05-6/2) grade to subglacial glaciofluvial sands. The preferred orientation of the clast fabric is stronger than the lodgement tills, with S_1 eigenvalues of 0.67–0.68 indicating clustered clast fabric (see Fig. 11). The main eigenvector (V_1) dips towards the W (295°), or to the S (189°), with the second most significant eigenvector (V_2) being perpendicular to the main one dipping towards the S (203°), or to the W (279°). Shell fragments reworked from older distal glaciomarine or marine sediments were found in unit PC05-6/1.

Subangular outlines of quartz grains in the medium sand fraction are most common in the subglacial melt-out till; sub-rounded and angular outlines are also quite common, but rounded grains are rare or absent. The relief of grains is mostly medium or sometimes high. Mechanical features are represented by very strong edge abrasion, many types of different steps and grooves (Fig. 10.8), conchoidal fractures, imbricated blocks and large breakage blocks (Fig. 10.8). Uprturned plates are common as well. Subrounded grains with common V-shaped pits (see Fig. 10.8) originated in more dynamic (marine or glaciofluvial) environments and were recycled from older sediments. Different types of pitting were also observed. Chemical features are present mainly by solution pits and limited silica precipitation, but other chemical features, such as extensive silica precipitation, adhering particles, and chemical V-shaped pits are present as well. Euhedral crystal overgrowths are absent.

4.1.3. Glaciofluvial sand of subglacial or englacial origin

Glaciofluvial sands are intercalated between lodgement tills, and have been found as individual layers 10–50 cm thick at the PC04-1, PC05-5, PC05-6 and PC05-7 sections. They are represented mostly by planar cross-bedded or ripple cross-laminated, medium- to well-sorted, medium- to coarse-grained sands with some gravel (Sp, Sr). They sometimes have erosional bases; coarsening upward is visible in some layers, and ripples are present in some units. They are mostly subglacial according to their position in the sedimentary sequence, but englacial origins could not be excluded. Granule- to pebble-sized

clasts are present depending on the degree of sorting of each layer with dominance of basaltic fragments.

4.2. Marine sediments

4.2.1. Glaciomarine debris-flow

Glaciomarine debris-flows are represented by massive clast-rich sandy to intermediate diamicrites (Dmm) at the PC05-2 section. Unit PC05-2/10 has a sharp undulated basal contact with underlying sandy sediments (see Fig. 8F), fining upwards and ploughing by larger boulders through the unit was documented. They probably represent displaced proximal glaciomarine diamicrites or even subglacial tills emplaced by slumping or debris flowages. The glaciomarine debris-flows are ~1.3 m thick and contain only 15–20% gravel clasts. JRVG basalt clasts dominate the clast lithology. The proportion of striated clasts (<25%) is lower than in subglacial tills. The shapes of gravel clasts are very similar to those of the clasts from subglacial tills, with mostly subangular to subrounded outlines and intermediate to high general sphericity. Nearly complete, sometimes articulated and well-preserved shells of *Austrochlamys anderssoni* were found in glaciomarine debris-flow units, suggesting their short transport distance.

4.2.2. Proximal to intermediate glaciomarine diamictonite to waterlain till

Glaciomarine diamictonite is the most common marine sediment in the Mendel Formation and was found in the PC04-1, PC04-2, PC05-1, PC05-2, PC05-9 and PC05-10 sections (see Fig. 8H). It is composed of massive or weakly stratified, clast-rich, sandy to intermediate diamicrites (Dmm, Dmws) with the thicknesses between 1 and >7 m. They consist of 20–35% gravel clasts with erratic clasts between 3 and 6%. 20–30% of striated clasts is present in glaciomarine diamictonite. Most of the gravel clasts are subangular to subrounded (80–90%) – rounded clasts are more common than angular ones. Basalt gravel clasts typically have intermediate to high values of general sphericity (c/a values between 0.4 and 0.7) with intermediate or slight rod affinity and C_{40} indices of 0–8% (see the individual glaciomarine diamicrites in Figs. 2–7). They are mostly homogeneous, but also show signs of cm-scale bedding. The base is mostly sharp and undulated and the material fines upward, the upper boundary being gradational. Cm-scale dropstones are located in the topmost 10 cm of the underlying laminated siltstones and sandstones. Silty drapes occur over some flat gravel clasts. Glaciomarine diamicrites also commonly

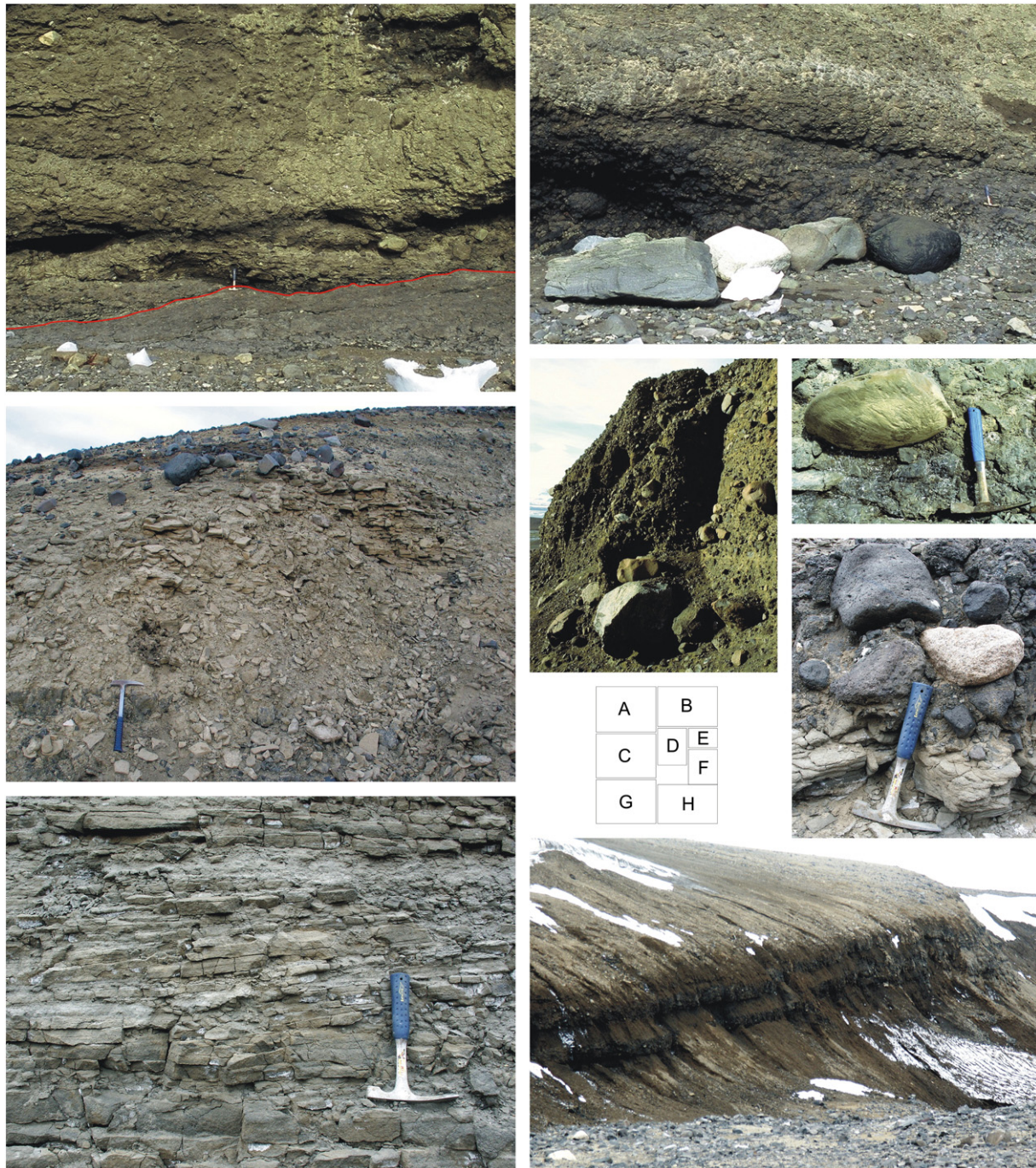


Fig. 8. Sedimentary lithofacies of the Mendel Formation. A. Erosional contact of basal glaciogenic sediments with underlying lava flow at the PC05-3 section. The erosional contact is redlined. B. Large erratic blocks originating from the Mendel Formation, on the beach close to the PC05-6 section. C. Tuffaceous horizontally laminated sandstone with exposed massive proximal glaciomarine diamictite to the left of the hammer at the PC04-2 section. D. Massive clast-rich diamictite with common erratics up to 1 m diameter in the bottom of the unit, with stratified sandy diamictite and smaller and more rounded erratics in the top at the PC05-8 section. The figure is 3.2 m high. E. Detail of striated Cretaceous silty sandstone concretion within the massive clast-rich intermediate diamictite at the PC05-6 section. F. Sharp undulating erosional basal contact of massive clast-rich glaciomarine debris-flow deposits with erratics and underlying tuffaceous laminated sandstone at the PC05-2 section. G. Tuffaceous laminated slightly inclined sandstone with 2–3 cm thick laminae at the PC05-2 section. H. General view of the lower part of the PC05-2 section (Section PC05-1 is located down-valley at the right-hand side of the same valley) with alternating tuffaceous horizontally laminated sandstone (lighter layers are covered mostly by scree) and massive clast-rich glaciomarine diamictites (darker layers with large clasts). The visible outcrop is ~45 m wide. The hammer in all figures is 28 cm long, with the exception of figure C, where the hammer is 40 cm long.

bear traces of reworking by sliding or slumping. They cannot always be differentiated from subaqueous glaciogenic (waterlain) tills.

Quartz sand grains have mainly subangular and angular outlines with predominant medium relief. Mechanical features are mainly edge abrasion, imbricated blocks (Fig. 10.5), large breakages and conchoidal fractures (Fig. 10.3 and 10.5). Other features present are different types of steps, grooves (Fig. 10.7) and ridges. Some older features such as different steps and V-shaped pits (Fig. 10.5 and 10.7)

are covered by a new generation of mechanical features (Fig. 10.3). All these features are typical of glacial environments; however, very abundant pitting, typical for marine environments, is present on the surface of some grains.

4.2.3. Tuffaceous horizontally laminated sandstone to siltstone

Horizontally laminated coarse- to fine-grained sandstones or coarse-grained siltstones (Sl, Fl), partly rhythmically bedded, comprise a

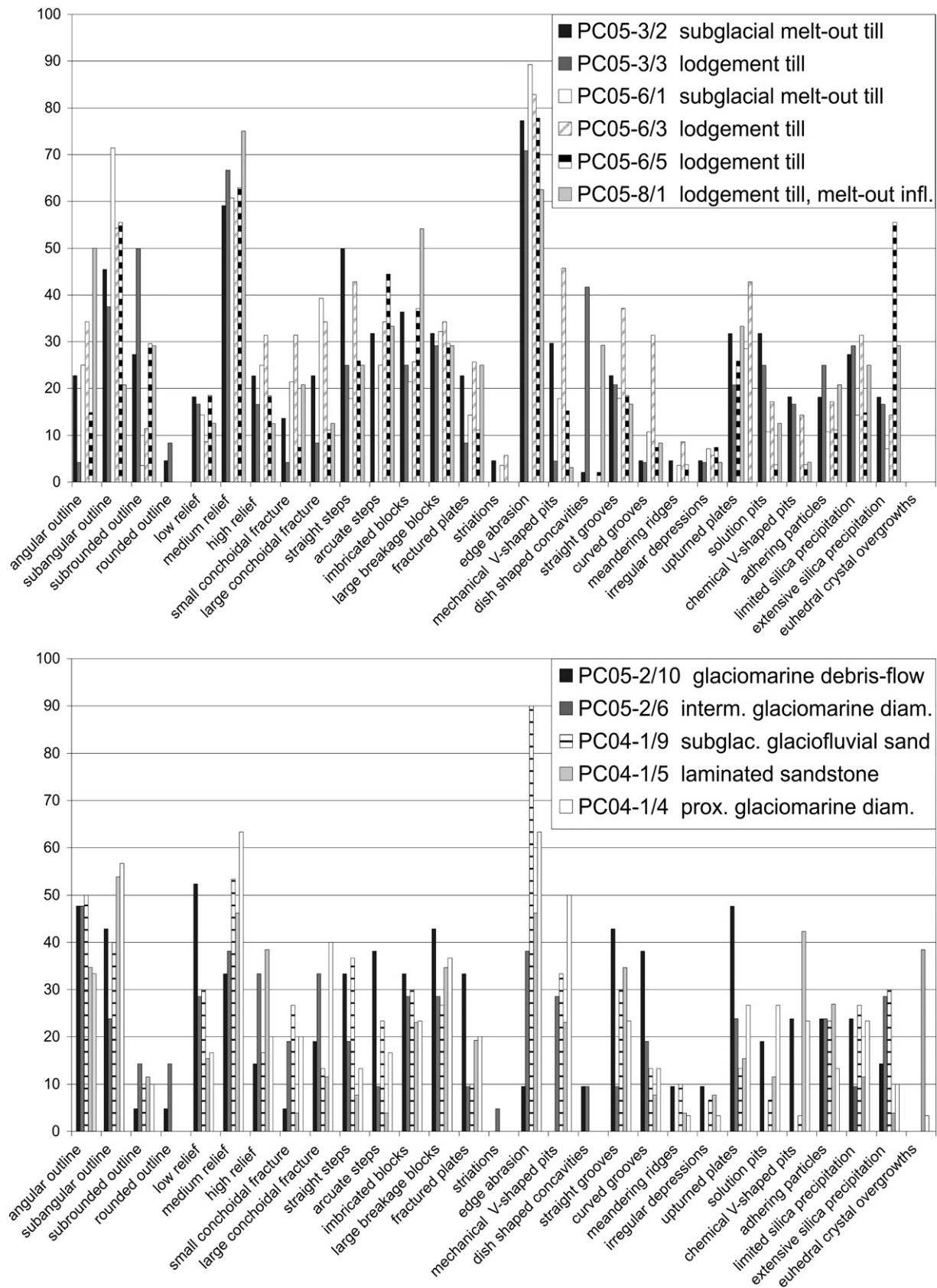


Fig. 9. Different quartz microtextures throughout the samples from different environmental settings of the Mendel Formation: those from terrestrial glacigenic sedimentary deposits in the upper part; and glaciofluvial, glaciomarine and marine sedimentary deposits in the lower part.

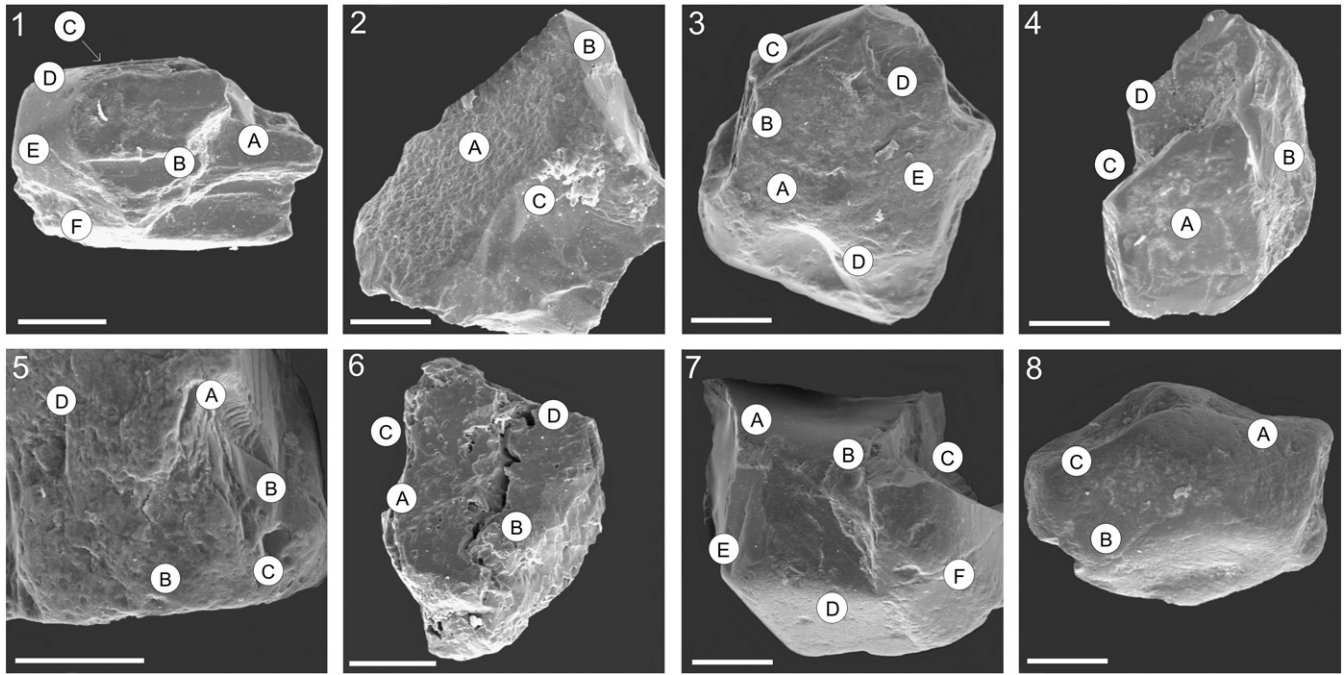


Fig. 10. Typical microtextures of quartz grains of the Mendel Formation. 1. Subrounded quartz grain with high relief from lodgement till with traces of melt-out processes; PC05-8/1; A – large breakage; B – upturned plates; C – subrounded outline; D – dish shaped concavity; E – straight step; F – imbricated block. 2. Angular quartz grain with medium relief from lodgement till with traces of melt-out processes; PC05-8/1; A – solution and chemical V-shaped pits; B – edge abrasion; C – adhering particles. 3. Subrounded quartz grain with medium relief from proximal glaciomarine sediment with slumping traces; PC04-1/4; A – V-shaped pits; B – large breakage; C – old conchoidal texture; D – imbricated blocks; E – adhering particles. 4. Subangular quartz grain with high relief and distinct phases of glacial transport from lodgement till with traces of melt-out processes; PC05-8/1; A – straight grooves and meandering ridges from the first glacial transport phase, filled by post-depositional limited silica precipitation; B – fresh small conchoidal fracture; C – edge abrasion; D – large breakage. 5. Subrounded quartz grain with medium relief from proximal glaciomarine sediment with slumping traces; PC04-1/4; A – conchoidal fracture; B – V-shaped pits and solution steps; C – imbricated blocks; D – straight step. 6. Subangular grain with medium relief from laminated pro-delta sediment; PC04-1/5; A – chemical V-shaped pits; B – edge abrasion; C – subangular outline; D – imbricated block. 7. Subrounded originally fluvial quartz grain crushed by glacial grinding from proximal glaciomarine sediment with slumping traces; PC04-1/4; A – sharp edge; B – small conchoidal fracture; C – large breakage; D – V-shaped pits; E – straight grooves; F – curved grooves. 8. Subrounded grain with medium relief from subglacial melt-out till; PC05-3/2; A – V-shaped pits; B – curved grooves; C – large breakage. White line at left bottom of each figure is 0.2 mm long.

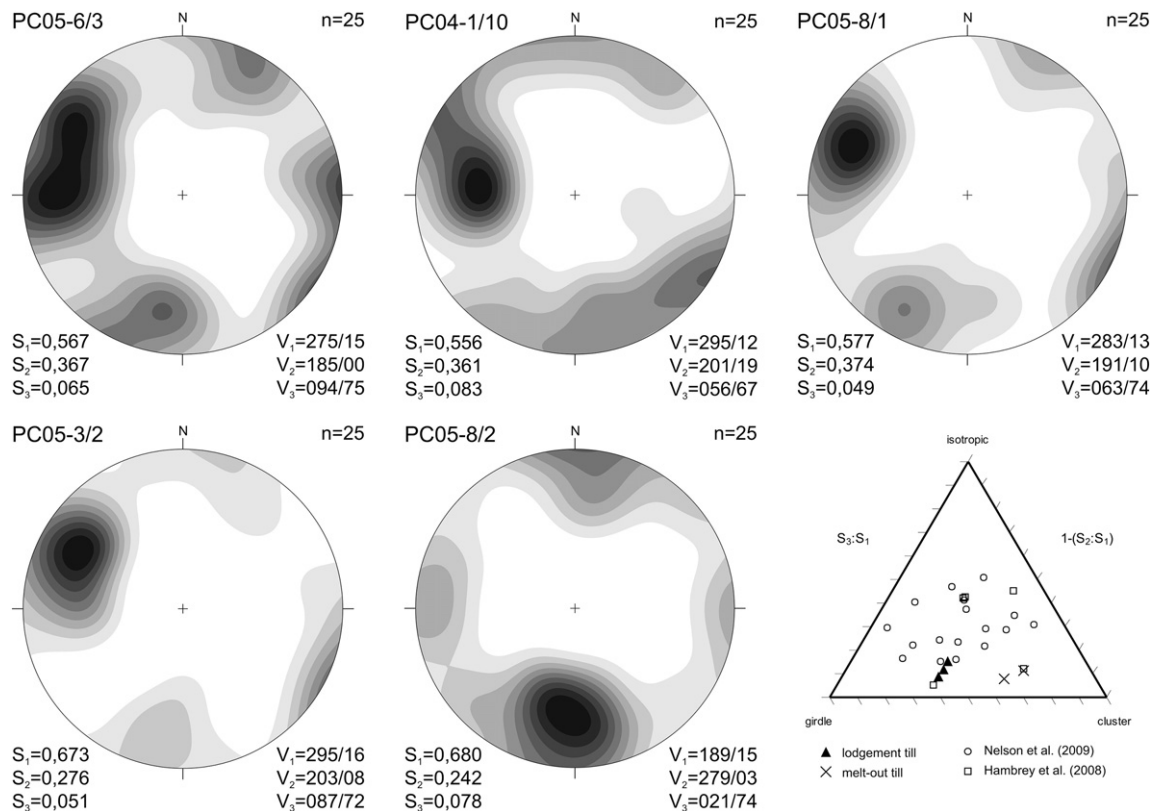


Fig. 11. Fabric shape of clasts from terrestrial subglacial till units of the Mendel Formation based on Benn's ternary diagram, compared with subglacial glaciogenic deposits of Hambrey et al. (2008) and glaciogenic debris flows of Nelson et al. (2009) from James Ross and Vega Islands.

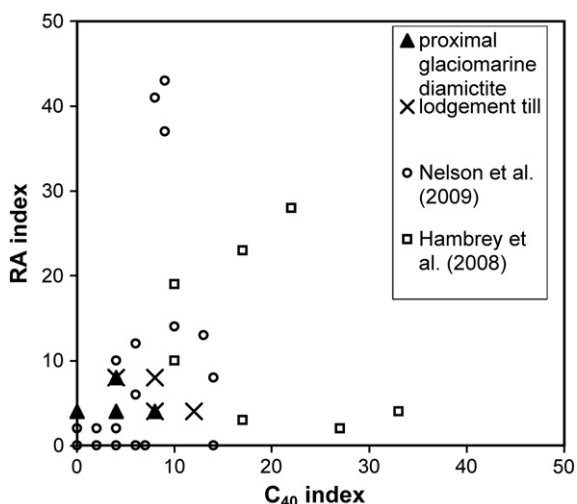


Fig. 12. Covariant plot of RA versus C_{40} indices for glaciomarine diamictites and lodgement tills from the Mendel Formation compared with stratified and massive diamictites of Hambrey et al. (2008) and glaciogenic debris flows of Nelson et al. (2009) from James Ross and Vega Islands.

significant part of the Mendel Formation (see Fig. 8C and G). They can be more than 5 m thick, with a gradational base and coarsening upward with common dropstones in the topmost 10 cm of each layer, but scarce in their distribution throughout. The top surfaces are sometimes erosional. Rhythmically bedded units (PC04-2/2 and PC04-2/4) contain laminae 1–10 cm thick, commonly 2–3 cm (see Fig. 8G). They are commonly planar-laminated, sometimes wavy or flaser-bedded, occasionally with loading structures. These tuffaceous laminites are composed mostly of sand and silt grains of quartz and basalt fragments, lower proportions of plagioclase, microcline, amphibole, clinopyroxene, epidote, palagonite glass, and some quartzite, olivine and mudstone with carbonate cement and small fragments of fossils indicating a dominant source in local Cretaceous sediments and Neogene basalts.

Morphological features on quartz grains of horizontally laminated sandstone and siltstone are represented mainly by subangular and angular outlines with medium to high relief, with some subrounded quartz grains. Mechanical features are poorly preserved and are mainly edge abrasion, imbricated blocks (Fig. 10.6) and large breakages. Conchoidal fractures are present but very badly preserved. Other features present are different types of steps, grooves, ridges and mechanical V-shaped pits (Fig. 10.6). The present mechanical and morphological features indicate previous glacial transport; the impact of the marine environment on the grain microtextures is limited. The most common and well preserved are chemical textural features such as chemical pitting and euhedral crystal overgrowths. Chemical solution, precipitation and adhering particles are present as well.

4.3. Lithofacies interpretation

The relative proportions of the different lithofacies have been calculated for the documented sections. The depositional sequence described here is composed mostly of massive to less stratified diamictites (nearly 76%). The sandy to silty lithofacies (Sp, Sl, Fl, Sh and Sr) are more important only in the middle part of the succession, representing 24% of the documented thickness. The individual lithofacies are interpreted in Figs. 2–7 and described above. The most common type of sedimentary deposits is lodgement till, partly with traces of melt-out processes (35%) and proximal to intermediate glaciomarine diamictites and waterlain till (33%). Horizontally laminated sandstone also forms a significant part (23%) of the succession. The other three sedimentary types (glaciomarine debris-flows, glaciofluvial sand and subglacial melt-out till) are less common and they account together for less than 10% of the succession. Sediments deposited in the

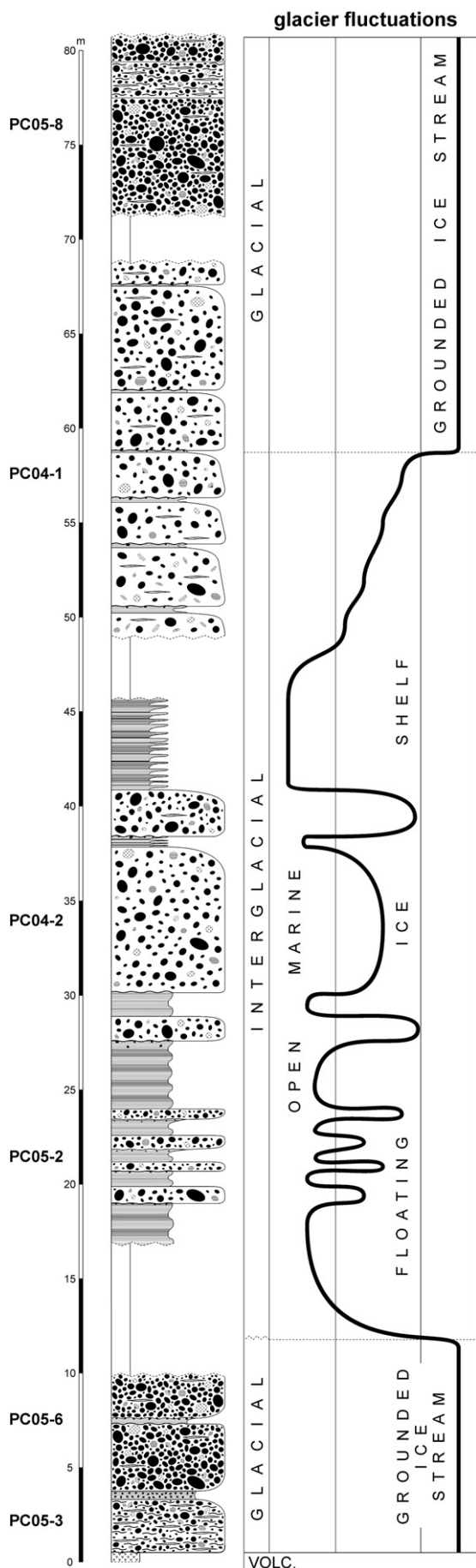
marine environment prevail slightly (59%) over terrestrial deposits (41%). The overall sedimentary thickness of the whole succession of the Mendel Formation exceeds 80 m.

Diamictite units contain 15–50% of gravel clasts; there is a slight difference in clast content between individual lithofacies. A higher proportion occurs in subglacial terrestrial facies, where there are 25–50% gravel clasts, with the average ~35%. Typically massive lodgement tills contain more gravel clasts than stratified subglacial melt-out tills. The proportion of gravel clasts in subaqueous diamictites is mostly 15–40%, with the average ~25%. The proportion of erratic gravels in diamictite units is mostly 1–6%, with an average of 4%. Clasts are mostly subangular to subrounded, always with more rounded clasts than angular ones. Striated clasts are more common in terrestrial glaciogenic sediments (30–45%) than in subaqueous diamictites (20–30%). The fabric shape in subglacial melt-out tills is rather high, with S_1 eigenvalues ~0.68 and moderate in lodgement tills with S_1 eigenvalues in the range 0.55–0.58 (see Fig. 11). The preferred orientation of clasts has been documented, especially for subglacial melt-out tills, where clast fabric shapes with an almost cluster pattern occur. Lodgement tills have girdle to cluster fabric shapes. All of the documented diamictite facies show very low C_{40} and RA indices; nevertheless, terrestrial subglacial tills have slightly higher values (see Fig. 12).

A rather high proportion of arcuate and straight steps, conchoidal fractures and breakage blocks on surfaces of studied sand grains in most subglacial till units show the importance of brittle fracture. However, edge abrasion, as the most common mechanical feature, together with the mostly sub-angular to sub-rounded outline of particles implies that brittle fractures originated in older comminution processes. The share of particles with edge abrasion is even higher in subglacial melt-out tills and in glaciofluvial sandy layers, than in lodgement tills. This relates to the amount of water present in the final deposition of the material. On the other hand, the portion of particles with edge abrasion is much lower for glaciomarine and marine deposits, with glaciomarine debris-flows having the lowest share. Glaciomarine debris-flow sand grains also mostly have low relief. Chemical textures are most important on grain surfaces in marine laminated sandstones. The most common is chemical pitting and euhedral crystal overgrowth. All these features are typical of very intense post-depositional weathering.

The lower contact of the Mendel Formation dips towards the W (295°) with an average dip of 15°. This contact is well exposed on the basalt surface, which is subglacially ploughed and striated. The clast fabric of the lowermost subglacial tills shows the main eigenvector (V_1) dipping in the same direction (see Fig. 11) as the striation on the underlying basalt surface. As the basalt was overridden by an advancing terrestrial glacier it is not possible to distinguish the glacier advance direction, as it may have been from E towards W or in opposite direction. However, according to rather high proportions of erratic rocks (up to 6%) originating from the AP we interpret the basal parts of the Mendel Formation as being subglacially deposited by an advancing ice tongue of the Antarctic Peninsula ice sheet (APIS). The W–E direction is dominant in clast fabrics of most of the terrestrial subglacial till units examined (see Fig. 11); the same orientation (276–278°) is also typical for dips of erosional bases of other subglacial tills (see Figs. 3 and 6). The orientation of laminae in marine tuffaceous siltstone and sandstone is towards the W and WNW (289–298°); most sharp or undulating bases of glaciomarine diamictite or subaqueous debris flows dip in the same direction (272–299°) with dips of 5°–11° (see Figs. 4–6). This shows that the sea invaded from the E during glacier retreat with floating ice shelf build-up.

Detailed study of sedimentary rock units of the Mendel Formation shows changes in the depositional environment through the evolution of the succession (see Fig. 13). Sedimentation started as terrestrial glaciogenic in the subglacial environment; subglacial tills are only sometimes intercalated by thin layers of sub/en-glacial glaciofluvial sandstone. The thickest middle part of the succession was



deposited in a glaciomarine to marine environment in distances changing from the glacier margin. The glaciomarine diamictites often bear evidences of subaqueous sliding and slumping; they have been deposited at various distances from the floating glacier margins with important ice-rafted component. The open marine laminated sandstone to siltstone was deposited in a pro-delta environment with a very limited glacial influence but are very probably coeval with the volcanic activity in the area, which was the most important source of the deposited material. Their top surfaces are sometimes erosional due to glacial or mass-movement erosion prior to the deposition of the subsequent unit, showing on a fluctuating floating glacier margin. The Mendel Formation terminates with terrestrial subglacial tills showing the advance of a grounded glacier.

5. Clast petrology

The gravel clasts found in the Mendel Formation can be divided in two groups according to their provenance; the most common are local JRI rocks including Cenozoic volcanic rocks and less common Cretaceous sedimentary rocks. The second group is made of erratic rocks originating from the AP and/or the Transantarctic and Ellsworth Mountains. The proportion of erratic gravels lies in the range of 1% to 6%, but it varies throughout the individual lithofacies (see above). The basic rock groups found in the gravel-to-boulder fraction in the Mendel Formation are summarised in Table 2 and shown in Fig. 14.

6. Dating of the Mendel Formation

The underlying basalt of Cape Lachman (sample JR-1) was dated using the ⁴⁰Ar/³⁹Ar method to determine the maximum age of deposition of the Mendel Formation. The basal part of the Mendel Formation rests directly on pillow lavas and overlying tuffs, which form a part of the Cape Lachman volcanic complex composed of pillow lavas, hyaloclastite tuffs to breccias and numerous dykes that yielded an isochron age of 5.85 ± 0.31 Ma (1 sigma including uncertainty on J value, 68% of the cumulative ³⁹Ar) with an ³⁶Ar/⁴⁰Ar intercept of 302.5 ± 20.4 and a MSWD of 1.45 (See Table 3 and Fig. 15). Both the intercept and the low MSWD indicate that this age is well constrained and may be used as the maximum age of the Mendel Formation.

Six shell samples were analysed for ⁸⁷Sr/⁸⁶Sr isotopic ratios (Table 4). The Sr isotopic data suggest that the sample taken from the PC04-1/2 unit is a reworked shell fragment from the underlying Cretaceous marine sediments. Its precise age cannot be derived from the Sr evolution curve, but based on the measured Sr isotopic ratio, it is between 84.9 and 130.2 Ma. There are four possible age intervals for this sample: 84.9–85.7 Ma, 97.2–104.0 Ma, 120.6–122.5 Ma, and 128.3–130.2 Ma. It is more likely that the dated shell fragment was reworked from the nearby Santa Marta Formation (Crame et al., 1991, 1999; Scasso et al., 1991), because it agrees with the age of belemnites dated at 85.5–86.1 Ma by McArthur et al. (2000) and rocks from other three above-mentioned age intervals can only be found in the western parts of JRI (Riding and Crame, 2002).

The other three pectinid shell samples were collected from terrestrial subglacial till units, and they were re-deposited from older glaciomarine or marine sediments. The ⁸⁷Sr/⁸⁶Sr age data indicate that the source sediments were deposited in an open marine interglacial setting in the lower Miocene (20.7–17.3 Ma). Sedimentary sequences of this age have not been found on JRI so far. The two samples from the PC05-1 section (correlated with PC05-2/10 unit) represent nearly complete, partly articulated and well-preserved shell fragments of *Austrochlamys anderssoni*. This indicates only limited transport of these

Fig. 13. Composite section of the Mendel Formation with the position of individual described sections and an interpretation of the glacial and interglacial conditions and glacier fluctuations.

Table 2

Main rock groups found within the gravel-to-boulder fraction of the Mendel Formation sediments. Minerals abbreviations according to Kretz (1983): (p) – phenocrysts or porphyroblasts, Op – opaque minerals.

Rock type	Provenance	Structures	Textures	Groundmass/matrix	Main minerals/clasts	Accessories	Notes
Olivine basalt	JRI	Compact to amygdaloidal	Intersertal, ophitic, porphyric, vesicular	Volcanic glass decomposed into lath-shaped Pl, serpentinized Ol, Srp	Ol (p), Pl, Cpx, Srp pseudomorphs, Spl and Ky inclusions	Mgt	Vesicles filled with zeolites, Chl and silt sediment xenoliths
Tuff, tuffite	JRI	Lappili	Clastic	Volcanic glass decomposed into mixture of phyllosilicates, fine Qtz clasts, Cpx, Pl, Kfs, Amp, Glt	Basalts, granites, contact-metamorphic biotite gneisses, Pl, Cpx, siltstones, greywackes, sandstone, Qtz		
Volcanic ash	JRI		Sandy clastic with granule admixture	Clay minerals	Volcanic rocks with ophitic texture, Pl, Px, Mgt, sandstones, sparite Qtz, Pl, Ep, Amp, Cpx, Ilm, chloritized Bt, carbonate-clay pellets		Calcareous test fragments
Siltstone to conglomerate	JRI		Silty to sandy clastic	Carbonate, sparite and clay minerals from decomposed volcanic glass			Carbonatized fossils
Granite, granodiorite, tonalite	AP batholith		Hypidiomorphic, granophyric	Mainly epigranular, sometimes porphyric medium-grained	Kfs, Pl, Qtz, Amp, Bt	Ap, Ms, Zrn, Ttn, Ep, Op	Alteration including sericitization, chloritization and epidotization
Gabbro, diorite	AP batholith		Medium-grained equigranular, poikilophitic	Mainly epigranular medium-grained	Pl, Qtz, Cpx, Amp, Hbl	Chl, Ttn, Hem, Ap, Ilm, Op, Ol pseudomorphs	Sericitization of Amp and Pl
Biotite paragneiss	AP batholith contact aureole	Banded	Fine-grained porphyroblastic with augen		Pl, Qtz, Bt, Kfs, Grt	Zrn, Ms, Chl, Ep, Cal, Op	
Biotite-cordierite paragneiss	AP batholith contact aureole		Heteroblastic to lepidogranoblastic, banded		Qtz, Pl, Bt, Kfs, Chl, sagenite, Crd	Zrn, Op	Migmatized
Chert	AP batholith contact aureole	Sometimes foliated	Micro-fibroganoblastic		Qtz, Bt, Ms, Crd pseudomorphs	Zrn, Cal, Ttn, Op	Secondary Chl
Phyllite	TPG	Banded, foliated	Micro-lepidogranoblastic		Qtz, Ms, Chl, Op		Crenulation cleavage
Biotite orthogneiss	AP basement, Transantarctic or Ellsworth Mts.	Banded augen, foliated	Granoblastic, lepidogranoblastic	Fine-grained	Pl, Kfs, Qtz, Bt, Zrn, Ms, Chl	Ilm, Ttn	Sericitization
Amphibolite	AP basement, Transantarctic or Ellsworth Mts.	Fine crystallized bands, weakly foliated	Nematogranoblastic		Amp, Ilm, Pl, Bt		

shells before their deposition and coeval living with subaqueous glacial deposition. The age may therefore be regarded as the depositional age for the middle part of the Mendel Formation at ~28 m, in the glaciomarine/marine part of the succession. The ages are $5.93 \pm 0.09 / -0.11$ and $5.65 \pm 0.15 / -0.24$ Ma and represent the only ages of the Mendel Formation valid for the glaciomarine/marine part.

7. Micropalaeontology

Biostratigraphical and palaeoenvironmental evidence of microfossils was limited by the extremely poor microfossil content of the Mendel Formation. Of the eight samples washed for microfossils, only two contained foraminifers (PC05-3/2, PC05-8/1), none of them contain any nannofossils. The total number of recovered foraminifers was just 3 specimens, together with one ostracod. The extreme scarcity is due to the terrestrial and glacial nature of the sedimentary deposits. The marine microfossils are reworked from older marine sediments. On the other hand, the samples from sediments interpreted here as being deposited in the pro-delta marine environment with less glacial influence (e.g. sample PC05-2/1), does not contain any obvious marine microfossils. A reason for that may be the low

salinity caused by melt-water input below and in front of the floating ice shelves during deposition of the rock.

Mineralised wood fragments are the most common fossil remnants. Most of them are coalified, but pyritised and silicified fragments also occur. The wood fragments apparently originate from different plant taxa. Fossil woods are commonly reported from the Upper Cretaceous on JRI (e.g. [Cantrill and Poole, 2005](#)), and this is a very probable source of wood fragments within the Mendel Formation, the other possibility may be the Miocene interglacial origin at the northern AP. However, further work is needed to solve the question of plant macro- and micro- (incl. the pollen and palynomorphs) fossils.

Among marine microfossils fragmentary, abraded and re-crystallised echinoid spines are most frequent. They are straight, narrow, possessing fine striation on the surface and radial structure on the cross section. Such types are characteristic of regular echinoids populating shallow seas worldwide.

Scarce foraminifers are represented by three taxa: *Hoeglundina asanoi* Matsunaga, *Nonionella bradii* (Chapman), and *Globocassidulina* sp. *Hoeglundina asanoi* was originally described by [Matsunaga \(1963\)](#) from the Pliocene of Japan and the specimen from sample PC05-3/2

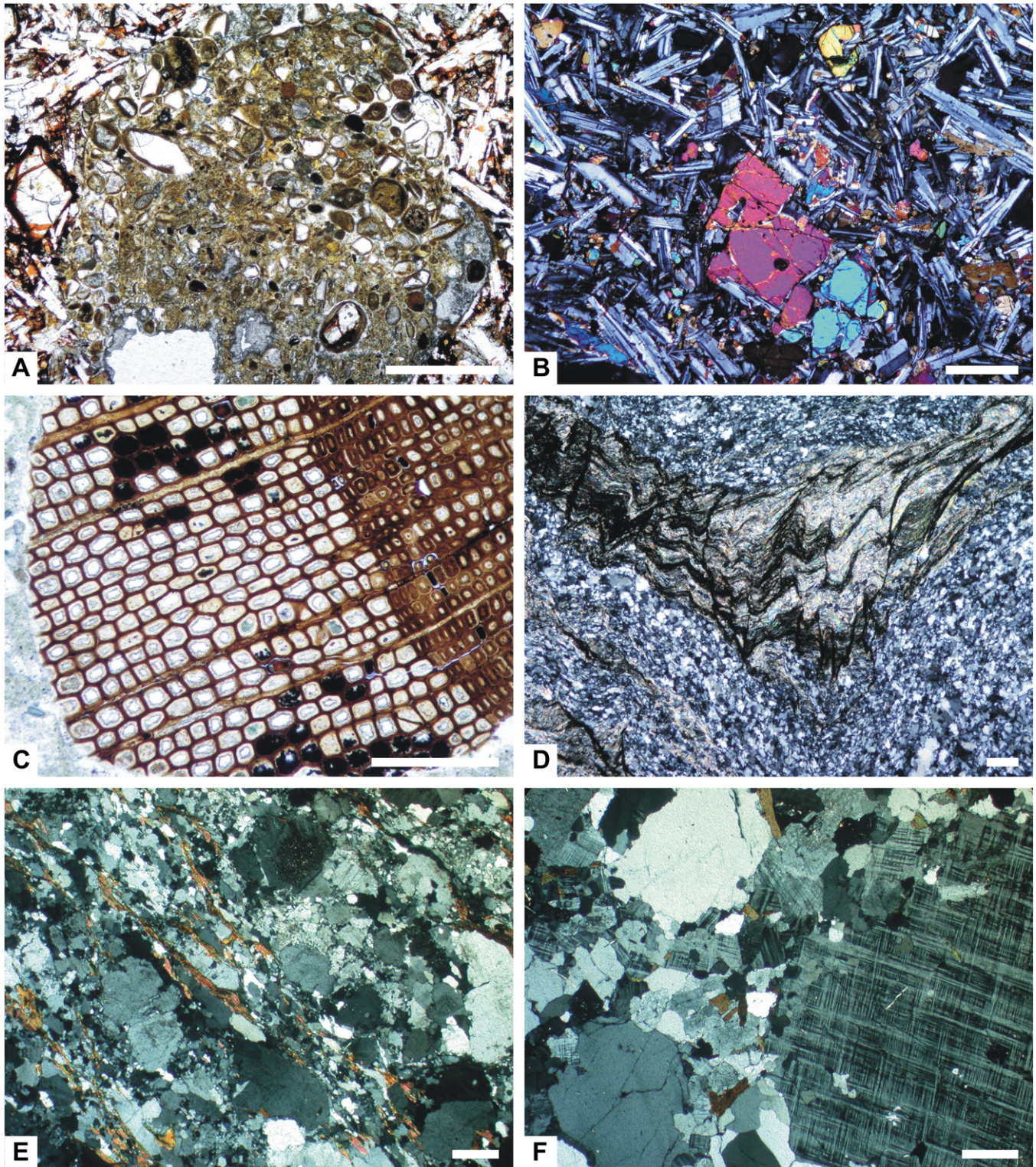


Fig. 14. Microphotographs of the typical local and erratic rocks from the Mendel Formation. A. Vesicle in basalt filled with silty sediments. B. Olivine basalt. C. Woody tissue constituting rarely interstitial material in pebbles from the Whisky Bay Formation. D. Phyllite with crenulation cleavage highlighted by organic pigment. E. Biotite orthogneiss. F. Muscovite-biotite granite. Scale bar at right bottom of each figure is 0.2 mm long.

corresponds well with the type description and figure of this species, though there are no recent records on its spatial and stratigraphic distribution. Generally, representatives of the genus live in cold and turbid waters on muddy substrates (also in Antarctic waters). The stratigraphic range of the genus is Cretaceous–Holocene.

Nonionella bradii was originally found in modern benthic communities of upper bathyal habitats of the Ross Sea. Specimens from

sample PC05-8/1 are close to the form from the Pecten conglomerate of Cockburn Island (Gaždicki and Webb, 1996). The stratigraphic range is Oligocene–Holocene.

Globocassidulina sp. is a damaged test with broken older chambers found in sample PC05-3/2 and differs from representatives of the genus common in the Austral realm. It is possible that the specimen represents juvenile *Cassidulinoides* sp. Cassidulinid foraminifers

Table 3

Complete data table for sample JR-1. ⁽¹⁾ ³⁹Ar ($\times 10^{-16}$ mol), ⁽²⁾ Cumulative ³⁹Ar gas released during the experiment (%), ⁽³⁾ %40* = % radiogenic ⁴⁰Ar of total ⁴⁰Ar released. J-value 0.005951. In bold steps 3–7, on which the calculated isochron age is based.

JR-1/step	40/39	38/39	37/39	36/39	³⁹ Ar ¹	F ³⁹ Ar ²	%40* ³	40*/39K	Age	± 1 sigma
1	4.642	0.037	0.293	0.014	3.843	1.17	11.60	0.54	5.77	1.36
2	1.879	0.024	0.300	0.005	35.207	11.85	22.20	0.42	4.48	0.15
3	1.174	0.021	0.260	0.002	57.535	29.32	46.50	0.55	5.86	0.14
4	0.956	0.020	0.232	0.001	54.990	46.01	55.50	0.53	5.69	0.05
5	0.929	0.020	0.212	0.001	45.194	59.73	56.40	0.52	5.61	0.12
6	0.938	0.019	0.290	0.001	37.729	71.18	56.70	0.53	5.70	0.07
7	1.038	0.020	0.278	0.002	28.399	79.81	49.60	0.51	5.52	0.09
8	1.151	0.019	0.249	0.002	20.895	86.15	60.20	0.69	7.43	0.13
9	1.500	0.019	0.290	0.003	26.530	94.20	38.30	0.58	6.17	0.20
10	2.482	0.022	0.305	0.006	10.390	97.36	34.20	0.85	9.09	0.50
11	3.342	0.022	0.416	0.009	8.711	100.00	22.80	0.76	8.17	0.90

represent dominant elements of Cenozoic benthic foraminifer communities of Antarctica.

The tests of *H. asanoi* and *Globocassidulina* sp. are filled with greenish, clay-like sediment that does not show any similarity to the lithology of the samples. This is a further indicator of possible reworking from older, very probably Cretaceous, sediments.

A single ostracod was recovered from sample PC05-3/2. It is a relatively well-preserved large right valve of *Rostrocytheridea* sp. Our species can be related to *Rostrocytheridea hamiltonensis* described recently by Fauth et al. (2003) from the Campanian of JRI, but it differs by possessing fine longitudinal ribs at the ventral side of the valve and by lacking any denticulation. Generally *Rostrocytheridea* is typical of the Cretaceous in the Austral realm.

Other marine microfossils recovered from the Mendel Formation were thick organic-walled brown-red cysts that can be assigned to the genus *Tasmanites* (Prasinophyta). Representatives of *Tasmanites* are reported from marine sediments through the Phanerozoic. Teleostean teeth and fragmentary sponge spicules rarely occur, but do not possess practical importance.

8. Formal lithostratigraphy

During the geological mapping in the northernmost Ulu Peninsula, sedimentary rocks representing former 'pecten conglomerates' of Andersson (1906) or 'tuffaceous conglomerates' of Nelson (1966) have been found and subsequently mapped in detail in the area between Cape Lachman, Berry Hill and Mendel Base (Fig. 1). They represent sediments deposited in open marine, glaciomarine and terrestrial glacial environments. The presence of these deposits was mentioned by various English and Argentinean geologists (e.g. Bibby, 1966; Hambrey and Smellie, 2006; Strelin et al., 1997), but they have not been studied in detail. A new formal name – Mendel Formation – is herein proposed for the sedimentary succession, because according to the data described here it does not correspond to any of the other Neogene sedimentary formations found on JRI (Drift Refugio San Carlos of Rabassa, 1983; Hobbs Glacier Formation of Pirrie et al., 1997; Belén Formation of Lirio et al., 2003; Gage Formation of Lirio et al., 2003; Terrapin Formation of Lirio et al., 2003).

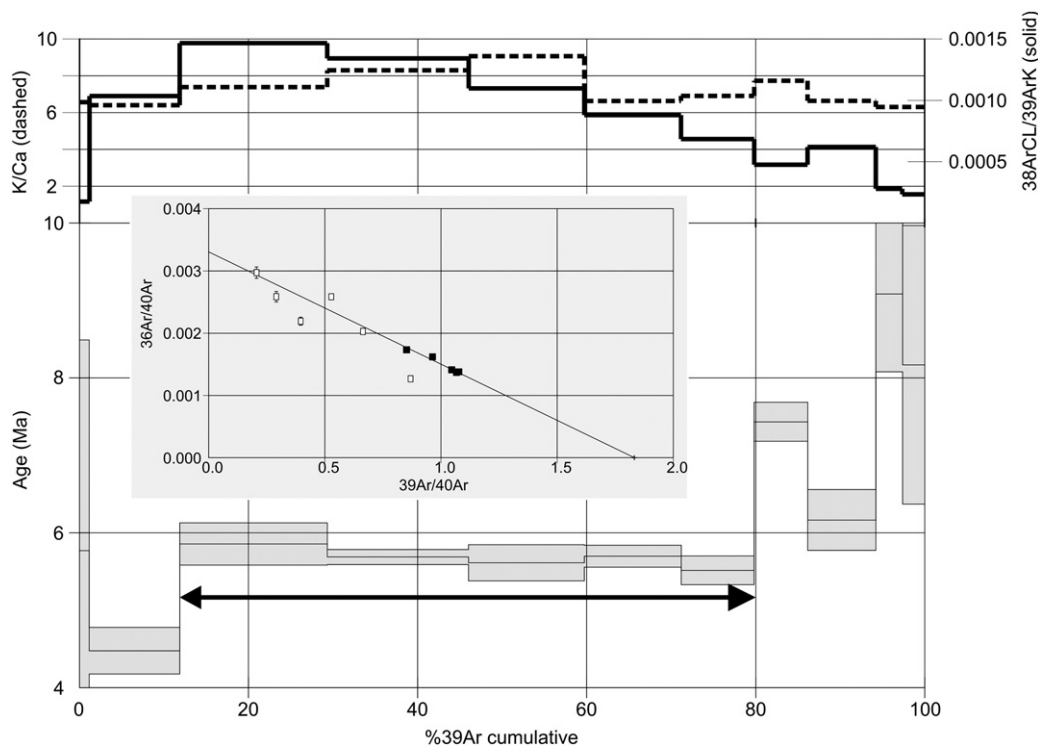


Fig. 15. Age spectrum for sample JR-1 (2 sigma error bars). Five steps cover 68% of cumulative ³⁹Ar. Isochron age (inset) for these steps is 5.85 ± 0.31 Ma (1 sigma, including uncertainty on J value). ³⁶Ar/⁴⁰Ar intercept 302.5 ± 20.4 with MSWD of 1.45. Top panel displays K/Ca (dashed) and ³⁸ArCl/³⁹ArK (solid) as a function of cumulative ³⁹Ar.

Table 4
Strontium isotopic data for shell fragments from the Mendel Formation. Ages calculated using the LOWESS version 3:10 of McArthur et al. (2001).

Sample	Geographical coordinates			$^{87}\text{Sr}/^{86}\text{Sr}$	± 2 sigma	Age Ma	Min. Ma	Max. Ma
	X	Y	Z [m a.s.l.]					
PC04-1/2	S 63° 48.3803'	W 57° 52.2605'	64	0.707436	0.000008	–	84.91	130.17
PC05-6/1	S 63° 48.0196'	W 57° 50.1290'	2	0.708429	0.000007	20.45	20.35	20.56
PC05-6/5	S 63° 48.0196'	W 57° 50.1290'	2	0.708645	0.000007	17.46	17.37	17.53
PC05-8/1	S 63° 48.3541'	W 57° 52.9455'	50	0.708569	0.000009	18.32	18.21	18.43
PC05-1a	S 63° 48.1222'	W 57° 52.5285'	23	0.708992	0.000008	5.93	5.84	6.02
PC05-1b	S 63° 48.1222'	W 57° 52.5285'	23	0.709012	0.000010	5.65	5.41	5.80

8.1. Derivation of the name

The Mendel Formation is named after the nearby Czech Johann Gregor Mendel Base, which is named for the famous scientist Johann Gregor Mendel – founder of the science of genetics – and is located on the Holocene marine terrace at the western tip of the sedimentary succession between Cape Lachman and Bibby Point, Ulu Peninsula, James Ross Island.

8.2. Boundaries and age

The Mendel Formation overlies Cretaceous marine strata (Whisky Bay and Hidden Lake Formations of the Gustav Group; Crame et al., 1991; Pirrie et al., 1997; Riding and Crame, 2002) in its southern and south-western part; at the neck of Cape Lachman in the north it overlies a subglacial volcanic sequence built of pillow lavas, hyaloclastite tuffs to breccias and dykes of one of the oldest phases of the JRIVG (Nelson, 1966; Smellie et al., 2008). This volcanic sequence was correlated with the Lachman Crags basal delta by Smellie et al. (2008) and a minimum age of 5.32 ± 0.16 Ma was reported based on the $^{40}\text{Ar}/^{39}\text{Ar}$ method. Unfortunately, the available sections of the Mendel Formation reveal only the contact with basalt at the PC05-3 section in the northern part of the sedimentary sequence (see Fig. 1). The contact between basalt and the overlying Mendel Formation diamictite at the PC05-3 section is erosional, sharp and undulating. At this time the maximum potential age of the Mendel Formation, based on dating the pillow lava (JR-1) using $^{40}\text{Ar}/^{39}\text{Ar}$ dating puts the age at 5.85 ± 0.31 Ma (Table 3, Fig. 15). This is older than the Davies Dome basal delta, which has an age of 5.04 ± 0.04 Ma as reported by Kristjánsson et al. (2005). Because the age reported by Smellie et al. (2008) for the Cape Lachman volcanic rocks (sample DJ.1715.1; 5.32 ± 0.16 Ma) is a minimum age, the validity of the correlation of the Cape Lachman volcanic rocks with the Lachman Crags basal delta (Smellie et al., 2008) cannot be evaluated based on these constraints alone. There are no outcrops showing the contact with Cretaceous rocks in the west; however, reworked Cretaceous fossils can be found in the lower diamictites of the PC04-1 section, indicating a position close to the Cretaceous basement.

The lower basaltic lava at Berry Hill, which marks the southern limit of the Mendel Formation, corresponds to the lava dated by Kristjánsson et al. (2005) to 5.04 ± 0.04 Ma in the southern part of Lachman Crags. Remnants of the basal Lachman Crags volcanic delta dated by Smellie et al. (2008) with a minimum age of 5.32 ± 0.16 Ma, also lie above the Mendel Formation. Numerous basaltic platy boulders up to 1 m wide and only few cm thick cover the surface of the Mendel Formation. As they are not present in the sediments of the Mendel Formation, they must represent remnants of a subaerial volcanic phase younger than the Mendel Formation, but older than the basal Lachman Crags delta.

In the east, at the neck of Cape Lachman, the sedimentary succession is covered by subglacial till with abundant erratic material (with granitoid boulders up to 3 m in the a-axis) derived from the AP and deposited during the last glacial maximum (MIS 2 prior to ~12 ka BP; unpublished data of the authors) by the (APIS) flowing through the northern Prince Gustav Channel towards Erebus and Terror Gulf

(Camerlenghi et al., 2001). Sediments of the Mendel Formation and Late Pleistocene to early Holocene glacial deposits are covered by (glacio)lacustrine deposits with a surface ~16–18 m asl on the eastern coast of the neck of Cape Lachman (Hjort et al., 1997; Ingólfsson et al., 1992). This ice-contact lacustrine deposition is of early Holocene age (~9.5 ka BP; Ingólfsson et al., 1992). A small westernmost part of the Mendel Formation is covered by a younger Holocene marine terrace (with a surface ~8–10 m asl), where the Mendel Base is built. In the south, the Mendel Formation is covered by Holocene blocky slope deposits with a small amount of matrix containing blocks of hyaloclastite breccias and basalts on the northern and northwestern slopes of Berry Hill, which in some places form protalus ramparts. The upper lower-lying part was transformed by paraglacial processes into sorted polygons on the flat surface and to sorted stripes and solifluction lobes on the slopes of Berry Hill. These forms and deposits are younger than the deglaciation of this area, which enabled the paraglacial activity. The age of the complete deglaciation is not known exactly, but there are data of lake sedimentation starting at ~9.5–6 ka BP from the wider area of the northern Ulu Peninsula (Hjort et al., 1997; Ingólfsson et al., 1992) and some data for neoglacial advances of local glaciers at ~5–4.2 ka BP (Björck et al., 1996; Hjort et al., 1997). The area covered by the Mendel Formation was not affected by any important neoglacial advance of local glaciers beside the small glacier on the southeastern slope of Berry Hill according to geological and geomorphological mapping (see Fig. 1). The upper contacts were not studied on any of the documented sections, as they are obscured by scree or there are no outcrops available in the relevant areas. The Mendel Formation occurs in the altitudinal range 0–155 m.

Two shells of *Austrochlamys anderssoni* from the PC05-1 section were dated using the Sr evolution curve for sea water (McArthur et al., 2001). This sample can be correlated with the PC05-2 section described, which is located in the same erosional valley. Shells are well preserved and nearly complete and originate from massive clast-rich sandy to intermediate diamictite. They were dated at $5.93 + 0.09/-0.11$ and $5.65 + 0.15/-0.24$ Ma (Table 4). Their physical appearance allows these ages to be interpreted as depositional ages of the studied part of the Mendel Formation. Beside samples of these ages, three other dateable pectinid shell samples were collected from terrestrial subglacial till units (PC05-6/1, PC05-6/5, PC05-8/1) of the Mendel Formation. Their $^{87}\text{Sr}/^{86}\text{Sr}$ ages fall into the lower Miocene (20.6–17.4 Ma), and they represent re-deposition from older sediments, as evidenced by their presence in terrestrial glacial deposits and their strongly fragmentary nature. The other dated shell fragment (from PC04-1/2 unit) represents reworked Cretaceous fossil material, a conclusion which is supported by abundant reworked macrofossil finds. According to the review of the ages listed above, the Mendel Formation was deposited during the late Miocene between 6.16 Ma and 5.23 Ma, taking into account 2 sigma uncertainties. Nevertheless, its deposition most probably occurred during a much shorter time in the middle of this interval.

8.3. Distribution

The extent of the Mendel Formation based on detailed geological mapping is shown in Fig. 1. It must continue below the Holocene marine terrace, where Mendel Base is built. Its distribution below sea

level is not known, but it could continue further west in Prince Gustav Channel and east in Herbert Sound. Sedimentary rocks of the Mendel Formation on the eastern cliff of the neck of the Cape Lachman are unfortunately buried by scree in the upper part and/or by snow-patches in the lower part of the cliff and they have therefore not been studied in detail.

8.4. Type section and thickness

The section with visible lower contact and subglacial tills is PC05-3, which lies close to sea level at the neck of Cape Lachman (S 63.79287°; W 57.81103°). Section PC05-2 (S 63.80385°; W 57.87252°), which was documented on slopes of a deeply incised stream valley in front of a small ice accumulation close to Mendel Base, represents the open marine and glaciomarine type section of the Mendel Formation. The maximum visible thickness is at the PC04-1 section, where a thickness of nearly 20 m was documented; the overall calculated sedimentary thickness of the whole succession must exceed 80 m (see Fig. 9). The base at the northern coast lies approximately at sea level, and the surface ascends to an altitude of ~155 m in its southern part on the slopes of Berry Hill. We know little about the nature of the base of the Mendel Formation, but it is possible that it is undulating and rises towards the S and SE. If the base of the Mendel Formation were planar, then the maximum thickness may reach 160 m, but this statement is rather speculative and may only be proved by geophysical methods.

8.5. Lithology

The Mendel Formation is composed of terrestrial glacial and glaciofluvial, glaciomarine and open marine sedimentary rocks. Terrestrial sedimentary deposits are composed of lodgement tills, subglacial melt-out tills and glaciofluvial sandstone, all of them subglacial or englacial in origin. Marine sedimentary deposits include glaciomarine debris-flows, glaciomarine diamictites to waterlain tills and tuffaceous horizontally laminated sandstones or siltstones. The whole succession constitutes a cycle of sedimentation starting as terrestrial glacial grading through glaciomarine sedimentation towards marine pro-delta sedimentation and back to terrestrial glacial deposition. A detailed lithofacies and sedimentary petrological description with environmental interpretation is given in the section "Lithofacies description and interpretation" (Section 4 above) and in Figs. 2–7.

8.6. Palaeontology

The present palaeontological finds are scarce. Macrofossil assemblages composed of well-preserved and nearly complete and sometimes articulated shells of *Austrochlamys anderssoni* were found in massive clast-rich sandy to intermediate diamictite (PC05-1 – correlated with PC05-2/10) and were used for $^{87}\text{Sr}/^{86}\text{Sr}$ dating. Their articulated and complete nature indicates short transport before deposition and coeval existence of these molluscs with subaqueous glacial deposition, and may therefore be used for dating the Mendel Formation. Other pectinid shell fragments were found only in the terrestrial glacial units (PC05-6/1, PC05-6/5, PC05-8/1) and must have been glacially reworked, as shown by their $^{87}\text{Sr}/^{86}\text{Sr}$ ages (see below). These collected fragments are too small (mostly less than 1 cm) to recognise species. Encrusting bryozoan colonies of up to few-cm large, calcified worm tubes and some barnacles were found on the surface of some basalt gravel clasts. Reworked Cretaceous bivalves and petrified wood are quite common, especially close to the base of the Mendel Formation where it overlies Cretaceous marine sedimentary rocks of the Whisky Bay and Hidden Lake Formations. The microfossil content of the formation consists of fragments of fossil wood (often coalified, less frequently pyritised or silicified), calcareous benthic foraminifers, echinoid spines, sponge spicules, rare *Tasmanites* cysts, fish teeth, and ostracods. Marine fossils

(foraminifers etc.) were obtained solely from terrestrial glacial units of the Mendel Formation and therefore represent reworked assemblages of a presently unknown origin. However, further work especially on palynomorphs, bryozoans and diatoms is needed to supplement the overall palaeontological knowledge of the Mendel Formation.

9. Discussion

9.1. Timing of Mendel Formation deposition

The prevailing olivine basalt and eruptive members of the basalt sequence found in the Mendel Formation relate to the early phase of volcanic activity at JRI (Nelson, 1966; Smellie, 1999; Smellie et al., 2008) during the late Miocene. The oldest dated in situ volcanic rocks in the northern part of the Ulu Peninsula are 6.16 ± 0.08 Ma old and form the Stickle Ridge lower delta (Smellie et al., 2008). The oldest $^{40}\text{Ar}/^{39}\text{Ar}$ ages of volcanic rocks from the JRIVG were from a basalt clast from diamictite at the Fjordo Belén, JRI dated at 9.2 ± 0.5 Ma (Jonkers et al., 2002) and a basalt clast from the Miocene diamictites of Seymour Island, recently dated using the $^{40}\text{K}/^{40}\text{Ar}$ method at 12.4 ± 0.5 Ma (Marenssi et al., 2010). In the northern Ulu Peninsula a basalt clast from glaciomarine diamictite was sandwiched between Cretaceous sediments of the Santa Marta Formation and JRIVG located close to the Crame Col and Medusa Cliffs dated using the $^{40}\text{K}/^{40}\text{Ar}$ method at 7.13 ± 0.49 Ma (Sykes, 1988).

The prevailing hyaloclastite tuff cone with associated pillow lavas of Cape Lachman is macroscopically different than any of the Lachman Crags volcanic rocks. At the time of the sedimentation of the Mendel Formation, the Lachman Crags basal delta did not exist, as volcanic rocks of the Lachman Crags lie stratigraphically above the Mendel Formation sedimentary rocks surrounding Berry Hill. Therefore, we assume that the Cape Lachman volcanic rocks predate and the Lachman Crags delta postdates the Mendel Formation, in spite of the $^{40}\text{Ar}/^{39}\text{Ar}$ ages lying within the 2 sigma uncertainty interval. Summarising these ages with the $^{87}\text{Sr}/^{86}\text{Sr}$ dating of pectinid shells, it seems that the possible depositional age of the Mendel Formation is 6.16–5.23 Ma; however, it was very probably deposited during a much shorter time in the middle of this interval, most likely between 5.9 and 5.4 Ma.

9.2. Stratigraphy and sedimentary environments

The Mendel Formation differs from the Hobbs Glacier Formation (Hambrey et al., 2008; Pirrie et al., 1997) not only in the thickness of the sedimentary succession, but especially by the cycle of sedimentation from terrestrial through glaciomarine and open marine back to terrestrial deposition. The thickness of the Mendel Formation (>80 m, or maybe up to 160 m) could be compared with the Cape Gage Formation of Lirio et al. (2003), for which the overall thickness may reach up to 50 m (J. M. Lirio, pers. comm. 2005) and with the thick conglomerate at Stickle Ridge (up to 150 m) or Rhino Cliffs (64 m) described by Nelson et al. (2009).

It is evident from the position of Mendel Formation above the Cape Lachman volcanic rocks, that Cape Lachman was a volcanic island separated from JRI by an ~2 km wide channel during the deposition of the Mendel Formation in the late Miocene. The other evidence for this is the recent marine terrace, which extends for some hundreds of meters on both sides of the neck of Cape Lachman during low tide. The exposure of pillow lava basalts and small Mendel Formation diamictite relics can be seen in the sea more than 200 m away from the coast and is only little covered by young marine mud drape. This terrace originated as a glacial erosional surface in volcanic rocks on which the sedimentary deposits of the Mendel Formation were deposited. The erosional signs below sea level are similar to those found at the base of the Mendel Formation (PC05-3 section) on the western cliff of the neck of Cape Lachman. The levelling of the surface is very probably marine in origin, but glacial erosion was the agent of

the final surface sculpting. Softer diamictites and tuffaceous sandstone have recently been removed from the sea floor on both sides of the Cape Lachman neck by marine erosion, and the former erosional surface has been re-exposed in the late Holocene after the fall of the sea level to its present position.

The tuffaceous sandstone to siltstone units in the Mendel Formation are not genetically connected with hyaloclastite breccias as Hambrey et al. (2008) demonstrated from other localities at James Ross Island. We interpret these tuffaceous horizontally laminated partly rhythmically bedded sandstone and siltstone, as being deposited in a marine pro-delta setting with low glacial influence as described by Pirrie and Sykes (1987). This interpretation is due to the presence of dropstones released from floating icebergs rather than the low concentration turbidity current deposition and direct ash-fall into the water body proposed later by Pirrie et al. (1997). Its tuffaceous nature and the presence of clasts of palagonite glass do not imply isochronism with local volcanic phases, but rather a reworking of volcanic material deposited in a setting rather distal from the volcanic source.

In addition to the prevailing local volcanic material incorporated in the Mendel Formation sediments, clasts of Cretaceous sediments of the James Ross Basin are also present. They consist of gravel conglomerates, which are likely to belong to coarse-grained members of the Whisky Bay Formation (late Albian to late Turonian). The conglomerates are accompanied by a variety of siltstone to sandstone and concretions derived from late Cretaceous formations of the James Ross Basin, which either underlies the Mendel Formation (Whisky Bay and Hidden Lake Formations) or lies in the vicinity (Santa Marta Formation). The reworking of material from underlying and/or adjoining Cretaceous formations was proved by the $^{87}\text{Sr}/^{86}\text{Sr}$ dating of reworked shells and by the presence of foraminifers and mineralised wood fragments of Cretaceous origin.

9.3. Provenance of erratic material

A small part of the gravel clasts (mostly 1–6%; but an important proportion of large boulders, see Fig. 8B) in the diamictites is not local, but of erratic rocks composed of magmatic, contact and regional metamorphic rocks. A broad spectrum of granitoids, diorites, tonalites and gabbros may be derived from the Antarctic Peninsula Batholith (Mount Reece and Mount Bradley being the closest area with their outcrops) see; e.g. Aitkenhead (1975), Leat et al. (1995), Scarrow et al. (1998). Biotite gneiss and chert are thought to form a contact aureole of the Antarctic Peninsula Batholith. This sequence is also likely to contain phyllite originating from the Trinity Peninsula Group, a low-grade flyshoid sequence of the Permian–Triassic accretion prism (e.g. Hyden and Tanner, 1981; Trouw et al., 1997).

The origin of gravels of regionally metamorphosed rocks, orthogneisses and amphibolites appears to be mysterious. High-grade metamorphic rocks form the Silurian–Triassic basement of the Antarctic Peninsula *sensu stricto* and are exposed in rare outcrops on the AP (cf. Hervé et al., 1996; Millar et al., 2002). However, the same rocks have also been found in more distant areas, such as the Transantarctic or Ellsworth Mountains, and have been glacially transported up to the South Shetland Islands (e.g. Polonez Cove and Cape Melville Formations on King George Island; Birkenmajer, 1987; Dingle and Lavelle, 1998; Troedson and Smellie, 2002). The far travelled erratics, for which the Transantarctic or Ellsworth Mountains origin is assumed, have very probably been transported in icebergs, which were carried along the AP by ocean currents controlled by the cyclonic Weddell Gyre (Diekmann and Kuhn, 1999; Swithinbank et al., 1980) from the Filchner-Ronne Ice Shelf area.

9.4. Ice dynamics and extent

Three-dimensional clast fabric analyses allowed differentiation between subglacial lodgement and melt-out tills. Subglacial melt-out

tills show generally better-developed cluster clast fabric shapes than lodgement tills, which have girdle to cluster fabric shapes. This difference has been shown in numerous studies around the world (e.g. Bennett et al., 1999; Dowdeswell and Sharp, 1986; Larsen and Piotrowski, 2003). Fabric shapes of subglacial till units in the Mendel Formation also differ from glacial debris flows described by Nelson et al. (2009), where more variable fabric shapes may be found. Terrestrial glacial units also have lower C_{40} and RA indices due to longer active (sub)glacial transport, which generally reduces disc- and rod-like clasts and decreases the general sphericity of highly spherical clasts (e.g. Bennett et al., 1997; Nývlt and Hoare, in press).

The generally high proportion of striated clasts (typically 30–45% in terrestrial glacial sediments and 20–30% in subaqueous diamictites), together with the degree of clast roundness (mostly subangular to subrounded) and the prevailing silty to fine-sandy matrix point mainly to warm-based glacier, active subglacial transport and glacial ploughing as very important factors (Benn and Evans, 1998). The importance of brittle fractures on quartz sand grains in subglacial tills, which is mostly attributed to glacier crushing (Mahaney, 1995), was shown by the study of quartz microtextures. However, they are commonly masked by edge abrasion, which is the most common mechanical superficial microtexture, implying that brittle fractures originated by older comminution processes. They are not necessarily only glacial in origin. Grain breakages require grain to grain contacts during transport (Fuller and Murray, 2002) and may have originated in submarine density flows at the slope or slope apron depositional environment (the environments interpreted for the underlying Cretaceous formations, e.g. Svojtka et al., 2009) or in the subaqueous volcanic environment. However, their glacial origin is more probable, and they are commonly taken to be indicators of subglacial transport at the base of thick ice sheets (with thickness usually greater than 1000 m), rather than under thin valley glaciers (Mahaney, 1995). Subsequent edge abrasion and clast rounding is connected with active transport of material in warm-based subglacial conditions, where surface abrasion causes particle rounding (Benn and Ballantyne, 1994) and fractures are less common due to less common grain to grain contacts owing to the water present. Edge abrasion is not typical of glaciomarine and marine deposits, where intense post-depositional weathering is present. This was shown to be typical of Late Pliocene glaciomarine deposits in the Bellingshausen Sea off Alexander Island by Cowan et al. (2008). They explained the presence of highly weathered grains, with a low proportion of crushed and abraded grains, by material transport by small glaciers that did not completely inundate the topography; therefore, much debris transported supraglacially or englacially was deposited without being substantially modified (Cowan et al., 2008). This shows a complex transport history of the grains before their final deposition; however, glacial transport dominates the shaping of the grain surfaces, as shown by Mahaney et al. (1996) for different tills from Antarctica.

Warm-based subglacial environments and active subglacial ploughing of particles were very common features for all Neogene glacial sequences associated with the JRIVG, as was recently shown by Hambrey and Smellie (2006), Smellie et al. (2006), Hambrey et al. (2008) and Nelson et al. (2009), but these environmental conditions differ strongly from recent cold-based local glaciers of JRI. Volcanic activity may have been an important agent for melting out of diamictites from basal glacier layers, as was mentioned by Smellie et al. (2006, 2008). An-other important observation is the mostly interglacial affinity of glaciomarine and marine sequences of the Mendel Formation due to the inheritance of well-preserved *Austrochlamys anderssoni*. The species of *Austrochlamys anderssoni* (formerly *Zygochlamys anderssoni* – see Jonkers, 2003 for a detailed taxonomic appraisal) disappeared from Antarctic waters at the Pliocene–Pleistocene transition (Berkman et al., 2004; Jonkers, 1998b), and lived mostly in relatively warmer conditions than were present around Antarctica during Quaternary interglacials and required ice-

free marine conditions even during winters (Berkman et al., 2004; Williams et al., 2010). The idea of glacier expansion during relatively warm periods was recently proposed also by Nelson et al. (2009) for other Neogene pectinid-bearing glacial debris flows from different parts of JRI. Williams et al. (2010) showed interglacial conditions for a slightly younger Cockburn Island Formation (4.4–4.8 Ma, McArthur et al., 2006) with sea-ice free NW Weddell Sea even during winter times.

The grounded APIS advanced eastwards through Prince Gustav Channel and crossed the northernmost part of the present JRI between the recent Lachman Crags and Cape Lachman. The form of Prince Gustav Channel evidently originated before the late Miocene, and its present pronounced glacial over-deepening with depth up to 1000 m in its northern part (Camerlenghi et al., 2001) resulted in multiple advances of grounded glaciers through this trough valley during the Neogene and Quaternary. The eastwards advance and transport of AP material is in good agreement with the results of Nelson et al. (2009), who found higher proportions of AP derived erratics (7–8%) in the NW part of JRI and interpreted some of these sediments (at Stoneley Point) as being deposited by the advancing APIS. Other locally derived glacial debris flows examined by Nelson et al. (2009) contain less than 1% of erratic gravel clasts originating from the AP and were deposited by a local ice cap or its outlets. Hambrey et al. (2008) found evidence of the advance of a grounded AP glacier at Pirrie Col on Vega Island, which lies towards the SE of the Mendel Formation. Sedimentary records from the marine and glaciomarine parts of the Mendel Formation show sea advance from the east connected with glacier retreat towards the AP area, which appeared during warmer interglacial conditions with rising sea level. The open marine warm conditions and deposition of marine laminites were interrupted by advancing and retreating floating ice shelves, below or in front of which glaciomarine diamictites and subaqueous debris flows were deposited. The floating ice shelf was later replaced by a grounded ice stream advancing in W–E direction.

9.5. Climatic implications

Sediments of Mendel Formation reveal changes in the depositional environment; sedimentation began as terrestrial glacial, continued as glaciomarine to marine and terminated again as terrestrial glacial. These changes also indicate different depositional distances from the glacier margin of the grounded glacier and floating ice shelf. Coeval volcanic activity may have been an important explanation for the high proportion of volcanic material deposited in the Mendel Formation, but probably not as important for the change of subglacial conditions to warm-based, as was proposed by Smellie et al. (2006, 2008). The warm-based or polythermal glacier regime was induced by the generally warmer late Miocene climate (Zachos et al., 2001a). On the other hand, the regional climatic trend revealed by opal depositional rate from Site 1095 in the Bellingshausen Sea off Alexander Island (Hillenbrand and Ehrmann, 2005) shows cooling during the latest Miocene between 6.9 and 5.6 Ma. However, the climate was still warmer than present, and cooling was interpreted only as a regional trend by Hillenbrand and Ehrmann (2005). Similarly, Billups (2002) concluded from isotopic records from Site 1088 at the Agulhas Ridge that the Southern Ocean cooled during the latest Miocene, and the cooling provided the initial conditions for the early Pliocene warming. Bart et al. (2005) reported at least 12 grounded glacier advances to the shelf edge on the opposite side of the AP during the Late Miocene (7.94–5.12 Ma); however, their closer correlation is not possible due to the lack of dating of the West AP grounding events.

Sedimentary deposits of the Mendel Formation show evidence of late Miocene climatic cyclicity. The benthic stable oxygen isotope record shows, that late Miocene and Pliocene climate change was driven by the obliquity cyclicity with a ~41 ka period (Lisiecki and Raymo, 2007; Naish et al., 2009). The Mendel Formation sedimentary

sequence is composed of at least two glacial and one interglacial interval; therefore, the whole sequence of the Mendel Formation may have been deposited within less than 100,000 years, but a longer time is more probable. The rapid warming between 5.6 and 5.0 Ma (Hillenbrand and Ehrmann, 2005) is connected with a major rise in relative sea level, which may be compared with the eustatic curve of Haq et al. (1987). Fielding et al. (2008) suggested a sea level rise of ~100 m between 6 and 5 Ma in the McMurdo Sound region. From the sedimentary record of the Mendel Formation, it can be shown that the sea level rise at the northern tip of the AP between glacial lowstand and interglacial highstand was >50 m during the late Miocene (5.9–5.6 Ma) and that it was followed by a subsequent sea level fall of at least the same magnitude.

Micro- and macro-fossils obtained from the sedimentary rocks of the Mendel Formation represent a pseudo-association – a mixture of reworked fossils from various sources. The allochthonous nature of the marine microfossils is evident from the fact that many of them were recovered from non-marine sedimentary rocks – in terrestrial subglacial tills. Neogene foraminifer and palynomorph assemblages in the area of JRI and the adjoining islands are described by Gaździcki and Webb (1996); Pirrie et al. (1997); Jonkers et al. (2002); Concheyro et al. (2005, 2007), and by Nelson et al. (2009). All of these authors report on re-working of late Cretaceous micro- and macro-fossils into Neogene microfossil associations, as is also the case in the Mendel Formation. Scarce foraminifer finds in the Mendel Formation may be stratigraphically assigned to the Oligocene–Miocene. It is probable that the source of some re-deposited microfossils is the same as the source of the pectinid bivalves (dated at 20.5–17.5 Ma). However, the original deposits have not been found in this part of Antarctica so far. The presence of pectinids is evidence of open marine interglacial sedimentation in this part of AP also during the early Miocene. This is concurrent with data from DSDP Site 270 log in the Ross Sea, where a limited amount of ice was recorded for the period 20–17 Ma (Barrett, 1999). A recent compilation of Cenozoic deep marine benthic foraminifer oxygen isotopic record (Zachos et al., 2001a) shows that after the first longer colder period during the Oligocene (34–26 Ma), a warmer period began with Late Oligocene warming at ~26 Ma, continued until the end of the mid-Miocene climatic optimum ~13 Ma ago (Zachos et al., 2001a) and was connected with high sea level (Haq et al., 1987) and higher atmospheric levels of CO₂ (Tripathi et al., 2009). This warmer period is interrupted only during the Mi-1 glaciation event centred at 23.0 Ma (Pälike et al., 2006; Roberts et al., 2003; Zachos et al., 2001b). The East Antarctic Ice Sheet was partial or ephemeral during this warm period and was re-established by 10 Ma, after the gradual cooling since ~14 Ma (Lewis et al., 2008; Williams et al., 2008; Zachos et al., 2001a). Further micro- and macro-palaeontological work is needed to resolve these questions.

10. Conclusions

Herewith we define the Mendel Formation, a sedimentary rock sequence appearing in the northern part of JRI, which is sandwiched between volcanic rocks of the JRIVG. Its broad depositional age is 6.16–5.23 Ma but was most likely to have been deposited between 5.9 and 5.4 Ma. This time interval is given by ages of underlying and overlying volcanic rocks supported by strontium dating of pectinid bivalves from the middle part of the sedimentary sequence. The Mendel Formation contains subglacial tills, sub- or en-glacial glacio-fluvial sediments, glaciomarine diamictites, subaqueous debris flows and laminated tuffaceous sandstone to siltstone, which were deposited in terrestrial glacial, glaciomarine and open marine sedimentary environments. Its cyclic sedimentary deposition in diverse sedimentary environments, position within the JRIVG, and its formation thickness (>80 m), differentiates the Mendel Formation from previously defined sedimentary formations cropping out in the JRI archipelago.

Glacier crushing features indicate subglacial transport at the base of an ice sheet more than 1000 m thick. These fractures are, however, mostly masked by edge abrasion and other features, which are connected with subglacial ploughing of material in warm-based subglacial conditions. Subglacial tills were deposited by a thick grounded APIS, with most of the material carried actively at the base of the glacier. These environmental and glaciological conditions differ strongly from the present cold-based local glaciers of JRI and the AP. The glaciomarine and marine sedimentary material was carried towards the glaciomarine/marine environment by small glaciers, where a significant part of the material was transported and deposited supraglacially or englacially without being modified by active glacial processes. The material was subsequently carried by a floating ice shelf and by calving icebergs towards the open sea away from the AP.

During the deposition of the Mendel Formation, Cape Lachman was a small volcanic island separated from JRI by an ~2 km wide channel. A significant proportion of erratics derived from AP or from southerly areas was found in diamictite units of the Mendel Formation. A grounded APIS advanced eastwards through the Prince Gustav Channel and crossed the northernmost part of the present JRI. The form of Prince Gustav Channel originated before the late Miocene and its present pronounced glacial over-deepening with depths up to 1000 m resulted in multiple grounded glacier advances through this valley during the Neogene and Quaternary. After the retreats of the grounded ice stream, the sea advanced from the E and the glacier margin began floating, building a small floating ice shelf, which was later replaced by a grounded ice stream advancing in W–E direction.

Coeval volcanic activity was an important factor inducing warm-based or polythermal subglacial conditions for other glaciomarine sediments at JRI, but not for the environmental changes documented in the Mendel Formation caused by global sea level fluctuation due to Antarctic ice sheet build up and decay connected with advances and retreats of the APIS and the associated ice shelf in the northern Prince Gustav Channel. This illustrates Late Miocene climatic cyclicity, which was driven by the obliquity ~41 ka period. The Mendel Formation sedimentary sequence is composed of at least two glacial periods and one interglacial period. The sea level rise at the northern tip of the AP based on the Mendel Formation sediments between the glacial lowstand and interglacial highstand was >50 m during the late Miocene and was followed by a subsequent sea level fall of at least the same magnitude. The age of the Mendel Formation is compatible with local relatively colder conditions in the Late Miocene with a climatic shift from a cooling period (6.9–5.6 Ma) towards the warming phase at the end of the Miocene and Early Pliocene (5.6–5.0 Ma) found in the circum-Antarctic waters around the AP.

The appearance of well-preserved, and sometimes articulated pectinid bivalves of *Austrochlamys anderssoni* in the glaciomarine part of the Mendel Formation is evidence for sedimentation during warm interglacial conditions with the open sea and on limited reworking of the shells before deposition. They therefore testify to less extensive glaciation along the AP in the Miocene “interglacials” and prevailing glaciomarine deposition below or in front of floating ice shelves. Reworked pectinid shells indicated an open marine “interglacial” condition in this part of AP during the Early to Mid Miocene (20.5–17.5 Ma). This timing is compatible with warmer circum-Antarctic and global conditions from different marine records. Unfortunately, the origin of the molluscs is obscure, as relevant sedimentary rocks have not been found on land.

Acknowledgements

This study was financially supported by R & D projects VaV/660/1/03 and VaV SP II 1a9/23/07 of the Ministry of the Environment of the Czech Republic. The fieldwork at JRI was undertaken by DN, JK, BM and PM mostly during the austral summer seasons of 2004, 2005 and 2007. We thank Juan Manuel Lirio for providing unpublished

information from his research on JRI and for help with searching the relevant Argentinean literature. Fuerza Aerea Argentina is also thanked for logistical support during the field campaigns. The work of LL was supported by Institutional research of the Institute of Geology, ASCR, v.v.i. no. Z 3013 0516. We are very grateful for the constructive comments of Mark Williams and both journal reviewers, which substantially helped to clarify this paper.

References

- Aitkenhead, N., 1975. The geology of the Duse Bay-Larsen Inlet area, North-East Graham Land. British Antarctic Survey Scientific Report 51. 62 pp.
- Andersson, J.G., 1906. On the Geology of Graham Land. Bulletin of the Geological Institution of the University of Uppsala 7, 19–71.
- Ballantyne, C.K., 1982. Aggregate clast form characteristics of deposits near the margins of four glaciers in the Jotunheimen Massif, Norway. Norsk Geografisk Tidsskrift 36, 103–113.
- Barrett, P., 1999. Antarctic climate history over the last 100 million years. Terra Antarctica Reports 3, 53–72.
- Bart, P.J., Egan, D., Warny, S.A., 2005. Direct constraints on Antarctic Peninsula Ice Sheet grounding events between 5.12 and 7.94 Ma. Journal of Geophysical Research 110, F04008.
- Benn, D.I., 1994. Fabric shape and the interpretation of sedimentary fabric data. Journal of Sedimentary Research A64, 910–915.
- Benn, D.I., Ballantyne, C.K., 1993. The description and representation of particle shape. Earth Surface Processes and Landforms 18, 665–672.
- Benn, D.I., Ballantyne, C.K., 1994. Reconstructing the transport history of glacial sediments: a new approach based on the co-variance of clast form indices. Sedimentary Geology 91, 215–227.
- Benn, D.I., Evans, D.J.A., 1998. Glaciers and glaciation. Arnold, London. 734 pp.
- Bennett, M.R., Hambrey, M.J., Huddart, D., 1997. Modification of clast shape in high-Arctic glacial environments. Journal of Sedimentary Research 67, 550–559.
- Bennett, M.R., Waller, R.L., Glasser, N.F., Hambrey, M.J., Huddart, D., 1999. Glacigenic clast fabrics: genetic fingerprint or wishful thinking? Journal of Quaternary Science 14, 125–135.
- Berkman, P.A., Cattaneo-Vietti, R., Chiantore, M., Howard-Williams, C., 2004. Polar emergence and the influence of increased sea-ice extent on the Cenozoic biogeography of pectinid molluscs in Antarctic coastal areas. Deep-Sea Research II 51, 1839–1855.
- Bibby, J.S., 1966. The stratigraphy of part of North-East Graham Land and the James Ross Island Group. British Antarctic Survey Scientific Report 53. 37 pp.
- Billups, K., 2002. Late Miocene through early Pliocene deep water circulation and climate change viewed from the sub-Antarctic South Atlantic. Palaeogeography, Palaeoclimatology, Palaeoecology 185, 287–307.
- Birkenmajer, K., 1982. Pliocene tillite-bearing succession of King George Island (South Shetland Island, Antarctica). Studia Geologica Polonica 74, 7–72.
- Birkenmajer, K., 1987. Oligocene–Miocene glacio-marine sequences of King George Island (South Shetland Islands), Antarctica. Palaeontologica Polonica 49, 9–36.
- Birkenmajer, K., Gaździcki, A., 1986. Oligocene age of the Pecten Conglomerate on King George Island, West Antarctica. Bulletin of the Polish Academy of Sciences, Earth Sciences 34, 219–226.
- Birkenmajer, K., Gaździcki, A., Gradziński, R., Kreuzer, H., Porebski, S.J., Tokarski, A.K., 1991. Origin and age of pectinid-bearing conglomerate (Tertiary) on King George Island, West Antarctica. In: Thomson, M.R.A., Crame, J.A., Thomson, J.W. (Eds.), Geological Evolution of Antarctica. Cambridge University Press, Cambridge, pp. 663–665.
- Björck, S., Olsson, S., Ellis-Evans, C., Håkansson, H., Humlum, O., de Lirio, J.M., 1996. Late Holocene palaeoclimatic records from lake sediments on James Ross Island, Antarctica. Palaeogeography, Palaeoclimatology, Palaeoecology 121, 195–220.
- Bull, P.A., 1986. Procedures in environmental reconstructions by SEM analysis. In: De Sieveking, G., Hart, U.B. (Eds.), The scientific study of Flint and Chert. Proceedings of the Fourth International Flint Symposium. Cambridge University Press, Cambridge, pp. 221–230.
- Camerlenghi, A., Domack, E., Rebesco, M., Gilbert, R., Ishman, S., Leventer, A., Brachfeld, S., Drake, A., 2001. Glacial morphology and post-glacial contourites in northern Prince Gustav Channel (NW Weddell Sea, Antarctica). Marine Geophysical Research 22, 417–443.
- Cantrill, D.J., Poole, I., 2005. Taxonomic turnover and abundance in Cretaceous to Tertiary wood floras of Antarctica: implications for changes in forest ecology. Palaeogeography, Palaeoclimatology, Palaeoecology 215, 205–219.
- Carrizo, H.G., Torielli, C.A., Strelin, J.A., Muñoz, C.E.J., 1998. Ambiente eruptivo del Grupo Volcánico Isla James Ross en Riscos Rink, Isla James Ross, Antártida. Revista de la Asociación Geológica Argentina 53, 469–479.
- Clark, N., Williams, M., Okamura, B., Smellie, J., Nelson, A., Knowles, T., Taylor, P., Leng, M., Zalasiewicz, J., Haywood, A., 2010. Early Pliocene Weddell Sea seasonality determined from bryozoans. Stratigraphy 7, 199–206.
- Colhoun, E.A., Kiernan, K.W., McConnell, A., Quilty, P.G., Fink, D., Murray-Wallace, C.V., Whitehead, J., 2010. Late Pliocene age of glacial deposits at Heidemann Valley, East Antarctica: evidence for the last major glaciation in the Vestfold Hills. Antarctic Science 22, 53–64.
- Concheyro, A., Adamonis, S., Salani, F.M., Lirio, J.M., 2005. La Formación Hobbs Glacier (Miocene Superior) en el sudeste de la Isla James Ross, Antártida: Localidades y

- contenido paleontológico. In: Actas del V° Simposio Argentino y I° Latinoamericano sobre Investigaciones Antárticas CD-ROM, Resumen Expandido N° 105GP, 4 pp.
- Concheyro, A., Salani, F.M., Adamonis, S., Lirio, J.M., 2007. Los depósitos diamictíticos cenozoicos de la cuenca James Ross, Antártida: Una síntesis estratigráfica y nuevos hallazgos paleontológicos. *Revista de la Asociación Geológica Argentina* 62, 568–585.
- Cowan, E.A., Hillenbrand, C.-D., Hassler, L.E., Ake, M.T., 2008. Coarse-grained terrigenous sediment deposition on continental rise drifts: a record of Plio-Pleistocene glaciation on the Antarctic Peninsula. *Palaeogeography, Palaeoclimatology, Palaeoecology* 265, 275–291.
- Crame, J.A., Pirrie, D., Riding, J.B., Thomson, M.R.A., 1991. Campanian–Maastrichtian (Cretaceous) stratigraphy of the James Ross Island area, Antarctica. *Journal of the Geological Society, London* 148, 1125–1140.
- Crame, J.A., McArthur, J.M., Pirrie, D., Riding, J.B., 1999. Strontium isotope correlation of the basal Maastrichtian Stage in Antarctica to the European and US biostratigraphic schemes. *Journal of the Geological Society, London* 156, 957–964.
- Czech Geological Survey, 2009. James Ross Island - Northern Part. Topographic map 1: 25 000. CGS, Praha.
- Dalrymple, G.B., Alexander, E.C., Lanphere, M.A., Kraker, G.P., 1981. Irradiation of samples for $^{40}\text{Ar}/^{39}\text{Ar}$ dating using the Geological Survey TRIGA reactor. *Geological Survey Professional Paper* 1176, 1–55.
- Del Valle, R.A., Marshall, P.A., Lirio, J.M., Camerlingo, E., 1987. Sobre la presencia del conglomerado con pecten en el fiordo Belen, isla James Ross. *Primera Reunion de Comunicaciones sobre Investigaciones Antárticas, Buenos Aires, 16 al 20 Noviembre 1987*. DNA, Buenos Aires.
- Diekmann, B., Kuhn, G., 1999. Provenance and dispersal of glacial–marine surface sediments in the Weddell Sea and adjoining areas, Antarctica: ice-rafting versus current transport. *Marine Geology* 158, 209–231.
- Dingle, R.V., Lavelle, M., 1998. Antarctic Peninsular cryosphere: Early Oligocene (c. 30 Ma) initiation and a revised glacial chronology. *Journal of the Geological Society, London* 155, 433–437.
- Dingle, R.V., McArthur, J.D., Vroon, P., 1997. Oligocene and Pliocene interglacial events in the Antarctic Peninsula dated using strontium isotope stratigraphy. *Journal of the Geological Society, London* 154, 257–264.
- Doktor, M., Gaździcki, A., Marensi, S.A., Porebski, S.J., Santillana, S.N., Vrba, A.V., 1988. Argentine–Polish geological investigations on Seymour (Marambio) Island, Antarctica. *Polish Polar Research* 9, 521–541.
- Dowdeswell, J.A., Sharp, M., 1986. Characterisation of pebble fabrics in modern terrestrial glacial sediments. *Sedimentology* 33, 699–710.
- Fang, A., Liu, X., Li, X., Huang, F., Yu, L., 2005. Cenozoic glacial sedimentary record in the Grove Mountains of East Antarctica. *Antarctic Science* 17, 237–240.
- Fauth, G., Seeling, J., Luther, A., 2003. Campanian (Upper Cretaceous) ostracods from southern James Ross Island, Antarctica. *Micropaleontology* 49, 95–107.
- Fielding, C.R., Whittaker, J., Henrys, S.A., Wilson, T.J., Naish, T.R., 2008. Seismic facies and stratigraphy of the Cenozoic succession in McMurdo Sound, Antarctica: implications for tectonic, climatic and glacial history. *Palaeogeography, Palaeoclimatology, Palaeoecology* 260, 8–29.
- Fuller, S., Murray, T., 2002. Sedimentological investigations in the forefield of an Icelandic surge-type glacier: implications for the surge mechanism. *Quaternary Science Reviews* 21, 1503–1520.
- Gaździcki, A., Webb, P.-N., 1996. Foraminifera from the Pecten Conglomerate (Pliocene) of Cockburn Island, Antarctic Peninsula. *Palaeontologia Polonica* 55, 147–174.
- Gaździcki, A., Tatur, A., Hara, U., Del Valle, R.A., 2004. The Weddell Sea Formation: post-Late Pliocene terrestrial glacial deposits on Seymour Island, Antarctic Peninsula. *Polish Polar Research* 25, 189–204.
- Graham, J.D., Midgley, N.G., 2000. Technical communication: graphical representation of particle shape using triangular diagrams: an excel spreadsheet method. *Earth Surface Processes and Landforms* 25, 1473–1477.
- Hambrey, M.J., 1994. *Glacial environments*. UCL Press, London, 296 pp.
- Hambrey, M.J., McKelvey, B., 2000. Major Neogene fluctuations of the East Antarctic ice sheet: Stratigraphic evidence from the Lambert Glacier region. *Geology* 28, 887–891.
- Hambrey, M.J., Smellie, J.L., 2006. Distribution, lithofacies and environmental context of Neogene glacial sequences on James Ross and Vega Islands, Antarctic Peninsula. In: Francis, J.E., Pirrie, D., Crame, J.A. (Eds.), *Cretaceous–Tertiary High-Latitude Palaeoenvironments*. James Ross Basin, Antarctica: Geological Society of London Special Publications 258, London, pp. 187–200.
- Hambrey, M.J., Webb, P.-N., Harwood, D.M., Krissek, L.A., 2003. Neogene glacial record from the Sirius Group of the Shackleton Glacier area, central Transantarctic Mountains, Antarctica. *Geological Society of America Bulletin* 115, 994–1015.
- Hambrey, M.J., Smellie, J.L., Nelson, A.E., Johnson, J.S., 2008. Late Cenozoic glacier–volcano interaction on James Ross Island and adjacent areas, Antarctic Peninsula region. *Geological Society of America Bulletin* 120, 709–731.
- Haq, B.U., Hardenbol, J., Vail, P.R., 1987. Chronology of fluctuating sea levels since the Triassic. *Science* 235, 1156–1167.
- Harwood, D.M., McMinn, A., Quilty, P.G., 2000. Diatom biostratigraphy and age of the Pliocene Sorsdal Formation, Vestfold Hills, East Antarctica. *Antarctic Science* 12, 443–462.
- Helland, P.E., Huang, P.-H., Diffendal, R.F., 1997. SEM Analysis of Quartz Sand Grain Surface Textures Indicates Alluvial/Colluvial Origin of the Quaternary “Glacial” Boulder Clays at Huangshan (Yellow Mountain), East-Central China. *Quaternary Research* 48, 177–186.
- Hennig, A., 1911. Le congrès de la Pleistocène à Pecten de l’île Cockburn: Wissenschaftliche Ergebnisse der Schwedischen Südpolar-Expedition, 1901–1903. *Geologie und Paläontologie* 3 (10), 1–73.
- Hervé, F., Lobato, J., Ugalde, I., Pankhurst, R.J., 1996. The geology of Cape Dubouzet, northern Antarctic Peninsula: continental basement to the Trinity Peninsula Group? *Antarctic Science* 8, 407–414.
- Hillenbrand, C.-D., Ehrmann, W., 2005. Late Neogene to Quaternary environmental changes in the Antarctic Peninsula region: evidence from drift sediments. *Global and Planetary Change* 45, 165–191.
- Hjort, C., Ingólfsson, Ó., Möller, P., Lirio, J.M., 1997. Holocene glacial history and sea-level changes on James Ross Island, Antarctic Peninsula. *Journal of Quaternary Science* 12, 259–273.
- Hyden, G., Tanner, P.W.G., 1981. Late Paleozoic–Early Mesozoic fore-arc basin sedimentary rocks at the Pacific margin in Western Antarctica. *Geologische Rundschau* 70, 529–541.
- Ingólfsson, Ó., Hjort, C., Björck, S., Smith, R.I.L., 1992. Late Pleistocene and Holocene glacial history of James Ross Island, Antarctic Peninsula. *Boreas* 21, 209–222.
- Ivany, L.C., Blake, D.B., Lohmann, K.C., Aronson, R.B., 2004. Eocene cooling recorded in the chemistry of La Meseta Formation molluscs, Seymour Island, Antarctic Peninsula. *GeoSur 2004 Proceedings, International Symposium on the Geology and Geophysics of the Southernmost Andes, the Scotia Arc and the Antarctic Peninsula*. Buenos Aires, 4 pp.
- Ivany, L.C., Van Simaey, S., Domack, E.W., Samson, S.D., 2006. Evidence for an earliest Oligocene ice sheet on the Antarctic Peninsula. *Geology* 34, 377–380.
- Jonkers, H.A., 1998a. The Cockburn Island Formation: Late Pliocene interglacial sedimentation in the James Ross Basin, northern Antarctic Peninsula. *Newsletters on Stratigraphy* 36, 63–76.
- Jonkers, H.A., 1998b. Stratigraphy of Antarctic late Cenozoic pectinid-bearing deposits. *Antarctic Science* 10, 161–170.
- Jonkers, H.A., 2003. Late Cenozoic–Recent Pectinidae (Mollusca: Bivalvia) of the Southern Ocean and Neighbouring Regions. *Monographs of Marine Mollusca* 5, Backhuys, Kerwerve, 125 pp.
- Jonkers, H.A., Lirio, J.M., Del Valle, R.A., Kelley, S.P., 2002. Age and environment of Miocene–Pliocene glaciomarine deposits, James Ross Island, Antarctica. *Geological Magazine* 139, 577–594.
- Kretz, R., 1983. Symbols for rock-forming minerals. *American Mineralogist* 68, 277–279.
- Kristjánsson, L., Gudmundsson, M.T., Smellie, J.L., McIntosh, W.C., Esser, R., 2005. Palaeomagnetic, $^{40}\text{Ar}/^{39}\text{Ar}$, and stratigraphical correlation of Miocene–Pliocene basalts in the Brandy Bay area, James Ross Island, Antarctica. *Antarctic Science* 17, 409–417.
- Larsen, N.K., Piotrowski, J.A., 2003. Fabric pattern in a basal till succession and its significance for reconstructing subglacial processes. *Journal of Sedimentary Research* 75, 725–734.
- Lawson, D.E., 1979. A comparison of the pebble orientations in ice and deposits of the Matanuska Glacier, Alaska. *Journal of Geology* 87, 629–645.
- Leat, P.T., Scarrow, J.H., Millar, I.L., 1995. On the Antarctic Peninsula batholith. *Geological Magazine* 132, 399–412.
- Lewis, A.R., Marchant, D.R., Ashworth, A.C., Hedenäs, L., Hemming, S.R., Johnson, J.V., Leng, M.J., Machlus, M.L., Newton, A.E., Raine, J.I., Willenbring, J.K., Williams, M., Wolfe, A.P., 2008. Mid-Miocene cooling and the extinction of tundra in the continental Antarctica. *Proceedings of the National Academy of Sciences of the United States of America* 105, 10676–10680.
- Lirio, J.M., Del Valle, R.A., 1997. Conglomerados con pecten (Miocene Superior y Pliocene Superior) en la isla J. Ross, Península Antártica. *IV Jornadas sobre Investigaciones Antárticas*. DNA, Buenos Aires, pp. 298–304.
- Lirio, J.M., Núñez, H.J., Bertels-Potok, A., Del Valle, R.A., 2003. Diamictos fosilíferos (Mioceno–Pleistoceno): Formaciones Belén, Gage y Terrapin en la isla James Ross, Antártida. *Revista de la Asociación Geológica Argentina* 58, 298–310.
- Lirio, J.M., Concheyro, A., Chaparro, M.A., Nývlt, D., Mlcoch, F., 2007. Diamictita Cabo Lamb, un nuevo depósito fosilífero marino Cenozoico en la Isla Vega, Península Antártica. In: Actas del VI° Simposio Argentino y III° Latinoamericano sobre Investigaciones Antárticas, Buenos Aires 10 al 14 de Septiembre de 2007. CD-ROM, Resumen Expandido N° GEORE818, Buenos Aires, 4 pp.
- Lisiecki, L.E., Raymo, M.E., 2007. Plio–Pleistocene climate evolution: trends and transitions in glacial cycle dynamics. *Quaternary Science Reviews* 26, 56–69.
- Mahaney, W.C., 1995. Glacial crushing, weathering and diagenetic histories of quartz grains inferred from scanning electron microscopy. In: Menzies, J. (Ed.), *Modern Glacial Environments – Processes, Dynamics and Sediments*, Glacial Environments, vol. 1. Butterworth-Heinemann, Oxford, pp. 487–506.
- Mahaney, W.C., Claridge, G., Campbell, I., 1996. Microtextures on quartz grains in tills from Antarctica. *Palaeogeography, Palaeoclimatology, Palaeoecology* 121, 89–103.
- Malagnini, E.C., Olivero, E.B., Rinaldi, C.A., Spikermann, Y.J.P., 1981. Aspectos geomorfológicos de la isla Vicecomodoro Marambio, Antártida. *VIII Congreso Geológico Argentino, Actas II, San Luis*, pp. 883–896.
- Marensi, S.A., Lirio, J.M., Stinco, L.P., Macchiavello, J.C., 1987. Informe preliminar acerca de diamictitas en el terciario de punta Redonda, Isla James Ross. *Primera Reunion de Comunicaciones sobre Investigaciones Antárticas, 16 al 20 Noviembre 1987*. DNA, Buenos Aires.
- Marensi, S.A., Casadio, S., Santillana, S.N., 2010. Record of Late Miocene glacial deposits on Isla Marambio (Seymour Island), Antarctic Peninsula. *Antarctic Science* 22, 193–198.
- Matsunaga, T., 1963. Benthonic smaller foraminifera from the oil fields of northern Japan. *Tohoku University, Scientific Reports, Ser. 2 (Geol.)*, v. 35, 2, Sendai.
- McArthur, J.M., Crame, J.A., Thirlwall, M.F., 2000. Definition of Late Cretaceous stage boundaries in Antarctica using strontium isotope stratigraphy. *Journal of Geology* 108, 623–640.
- McArthur, J.M., Howarth, R.J., Bailey, T.R., 2001. Strontium isotope stratigraphy: LOWESS Version 3. Best-fit line to the marine Sr-isotope curve for 0 to 509 Ma and accompanying look-up table for deriving numerical age. *Journal of Geology* 109, 155–169.
- McArthur, J.M., Rio, D., Massari, F., Castradori, D., Bailey, T.R., Thirlwall, M., Houghton, S., 2006. A revised Pliocene record for marine- $^{87}\text{Sr}/^{86}\text{Sr}$ used to date an interglacial

- event recorded in the Cockburn Island Formation, Antarctic Peninsula. *Palaeogeography, Palaeoclimatology, Palaeoecology* 242, 126–136.
- McDougall, I., Harrison, T.M., 1999. *Geochronology and thermochronology by the $^{40}\text{Ar}/^{39}\text{Ar}$ method*, Oxford Monographs on Geology and Geophysics 9, Second ed. Oxford University Press, New York. 269 pp.
- McKelvey, B.C., Hambrey, M.J., Harwood, D.M., Mabin, M.C.G., Webb, P.-N., Whitehead, J.M., 2001. The Pogodroma Group—a Cenozoic record of the East Antarctic Ice Sheet in the northern Prince Charles Mountains. *Antarctic Science* 13, 455–468.
- Millar, I.L., Pankhurst, R.J., Fanning, C.M., 2002. Basement chronology of the Antarctic Peninsula: recurrent magmatism and anatexis in the Palaeozoic Gondwana Margin. *Journal of the Geological Society, London* 159, 145–156.
- Moncrieff, A.C.M., 1989. Classification of poorly-sorted sedimentary rocks. *Sedimentary Geology* 65, 191–194.
- Naish, T., Powell, R., Levy, R., Wilson, G., Scherer, R., Talarico, F., Krissek, L., Niessen, F., Pompilio, M., Wilson, T., Carter, L., DeConto, R., Huybers, P., McKay, R., Pollard, D., Ross, J., Winter, D., Barrett, P., Browne, G., Cody, R., Cowan, E., Crampton, J., Dunbar, G., Dunbar, N., Florindo, F., Gebhardt, C., Graham, I., Hannah, M., Hansaraj, D., Harwood, D., Helling, D., Henrys, S., Hinnov, L., Kuhn, G., Kyle, P., Läufer, A., Maffioli, P., Magens, D., Mandernack, K., McIntosh, W., Millan, C., Morin, R., Ohneiser, C., Paulsen, T., Persico, D., Raine, I., Reed, J., Riesselman, C., Sagnotti, L., Schmitt, D., Sjunneskog, C., Strong, P., Taviani, M., Vogel, S., Wilch, T., Williams, T., 2009. Obliquity-paced Pliocene West Antarctic ice sheet oscillations. *Nature* 458, 322–328.
- Nelson, P.H.H., 1966. The James Ross Island Volcanic Group of North-East Graham Land. *British Antarctic Survey Scientific Report* 54. 62 pp.
- Nelson, A.E., Smellie, J.L., Hambrey, M.J., Williams, M., Vautravers, M., Salzmann, U., McArthur, J.M., Regelous, M., 2009. Neogene glaciogenic debris flows on James Ross Island, northern Antarctic Peninsula, and their implications for regional climate history. *Quaternary Science Reviews* 28, 3138–3160.
- Nordenskjöld, O., 1905. Petrographische Untersuchungen aus dem westantarktischen Gebiete. *Bulletin of the Geological Institution of the University of Uppsala* 6, 234–246.
- Nývlt, D., Hoare, P.G., in press. Petrology, provenance and shape of clasts in the glaciofluvial sediments of the Mníšek member, northern Bohemia, Czechia. *Journal of Geological Sciences, Anthropozoic*.
- Pälike, H., Norris, R.D., Herrle, J.O., Wilson, P.A., Coxall, H.K., Lear, C.H., Shackleton, N.J., Tripati, A.K., Wade, B.S., 2006. The heartbeat of the Oligocene climate system. *Science* 314, 1894–1898.
- Pirrie, D., Sykes, M.A., 1987. Regional significance of proglacial delta-front reworked tuffs, James Ross Island area. *British Antarctic Survey Bulletin* 77, 1–12.
- Pirrie, D., Crame, J.A., Riding, J.B., 1991. Late Cretaceous stratigraphy and sedimentology of Cape Lamb, Vega Island, Antarctica. *Cretaceous Research* 12, 227–258.
- Pirrie, D., Crame, J.A., Riding, J.B., Butcher, A.R., Taylor, P.D., 1997. Miocene glaciomarine sedimentation in the northern Antarctic Peninsula region: the stratigraphy and sedimentology of the Hobbs Glacier Formation, James Ross Island. *Geological Magazine* 136, 745–762.
- Powers, M.C., 1953. A new roundness scale for sedimentary particles. *Journal of Sedimentary Petrology* 23, 117–119.
- Quilty, P.G., Lirio, J.M., Jiliet, D., 2000. Stratigraphy of the Pliocene Sørsdal Formation, Marine Plain, Vestfold Hills, East Antarctica. *Antarctic Science* 12, 205–216.
- Rabassa, J., 1983. Stratigraphy of the glaciogenic deposits in Northern James Ross Island, Antarctic Peninsula. In: Evenson, E., Schlüchter, C., Rabassa, J. (Eds.), *Tills and related deposits*. A.A. Balkema, Rotterdam, pp. 329–340.
- Riding, J.B., Crame, J.A., 2002. Aptian to Coniacian (Early-Late Cretaceous) palynostratigraphy of the Gustav Group, James Ross Basin, Antarctica. *Cretaceous Research* 23, 739–760.
- Roberts, A.P., Wilson, G.S., Harwood, D.M., Verosub, K.L., 2003. Glaciation across the Oligocene-Miocene boundary in southern McMurdo Sound, Antarctica: new chronology from the CIROS-1 drill hole. *Palaeogeography, Palaeoclimatology, Palaeoecology* 198, 113–130.
- Scarrow, J.H., Leat, P.T., Wareham, C.D., Millar, I.L., 1998. Geochemistry of mafic dykes in the Antarctic Peninsula continental-margin batholith: a record of arc evolution. *Contributions to Mineralogy and Petrology* 131, 289–305.
- Scasso, R.A., Olivero, E.B., Buatois, L.A., 1991. Lithofacies, biofacies, and ichnoassemblage evolution of a shallow submarine volcanoclastic fan-shelf depositional system (Upper Cretaceous, James Ross Island, Antarctica). *Journal of South American Earth Sciences* 4, 239–260.
- Smellie, J.L., 1999. Lithostratigraphy of Miocene-recent, alkaline volcanic field in the Antarctic Peninsula and eastern Ellsworth Land. *Antarctic Science* 11, 362–378.
- Smellie, J.L., McArthur, J.M., McIntosh, W.C., Esser, R., 2006. Late Neogene interglacial events in the James Ross Island region, northern Antarctic Peninsula, dated by Ar/Ar and Sr-isotope stratigraphy. *Palaeogeography, Palaeoclimatology, Palaeoecology* 242, 169–187.
- Smellie, J.L., Johnson, J.S., McIntosh, W.C., Esser, R., Gudmundsson, M.T., Hambrey, M.J., van Wyk de Vries, B., 2008. Six million years of glacial history recorded in volcanic lithofacies of the James Ross Island Volcanic Group, Antarctic Peninsula. *Palaeogeography, Palaeoclimatology, Palaeoecology* 260, 122–148.
- Sneed, E.D., Folk, R.L., 1958. Pebbles in the lower Colorado River, Texas: a study in particle morphogenesis. *Journal of Geology* 66, 114–150.
- Steiger, R.H., Jäger, E., 1977. Subcommittee on geochronology: convention on the use of decay constants in geo- and cosmochronology. *Earth and Planetary Science Letters* 36, 359–362.
- Strelin, J.A., Muñoz, C.E., Torielli, C.A., Carrizo, H.G., Medina, F.A., 1997. Las Diamicitas de la isla James Ross, Antártida: Origen y probable relación con "Conglomerado con Pecten". IV Jornadas sobre Investigaciones Antárticas. DNA, Buenos Aires, pp. 328–335.
- Stroeven, A.P., 1997. The Sirius Group of Antarctica: age and environments. In: Ricci, C.A. (Ed.), *The Antarctic region: geological evolution and processes*. Terra Antarctica Publications, Siena, pp. 747–761.
- Svojtka, M., Nývlt, D., Murakami, M., Vrávová, J., Filip, J., Mixa, P., 2009. Provenance and post-depositional low-temperature evolution of the James Ross Basin sedimentary rocks (Antarctic Peninsula) based on fission track analysis. *Antarctic Science* 21, 593–607.
- Swithinbank, C., McClain, P., Little, P., 1980. Drift tracks of Antarctic icebergs. *Polar Record* 18, 495–501.
- Sykes, M.A., 1988. New K–Ar age determinations on the James Ross Island Volcanic Group, North-East Graham Land, Antarctica. *British Antarctic Survey Bulletin* 80, 51–56.
- Tripati, A.K., Roberts, C.D., Eagle, R.A., 2009. Coupling of CO₂ and ice sheet stability over major climate transitions of the last 20 million years. *Science* 326, 1394–1397.
- Troedson, A.L., Smellie, J.L., 2002. The Polonez Cove Formation of King George Island, Antarctica: stratigraphy, facies and implications for mid-Cenozoic cryosphere development. *Sedimentology* 49, 277–301.
- Trouw, R.A.J., Passchier, C.W., Simoes, L.S.A., Andreis, R.R., Valeriano, C.M., 1997. Mesozoic tectonic evolution of the south Orkney microcontinent, Scotia arc, Antarctica. *Geological Magazine* 134, 383–401.
- Webb, P.-N., Harwood, D.M., Mabin, M.C.G., McKelvey, B.C., 1996. A marine and terrestrial Sirius Group succession, middle Beardmore Glacier–Queen Alexandra Range, Transantarctic Mountains, Antarctica. *Marine Micropalaeontology* 27, 273–297.
- Williams, M., Siveter, D.J., Ashworth, A.C., Wilby, P.R., Horne, D.J., Lewis, A.R., Marchant, D.R., 2008. Exceptionally preserved lacustrine ostracods from the Middle Miocene of Antarctica: implications for high-latitude palaeoenvironment at 77° south. *Proceedings of the Royal Society B* 275, 2449–2454.
- Williams, M., Nelson, A.E., Smellie, J.L., Leng, M.J., Johnson, A.L.A., Jarram, D.R., Haywood, A.M., Peck, V.L., Zalasiewicz, J., Bennett, C., Schöne, B.R., 2010. Sea ice extent and seasonality for the Early Pliocene northern Weddell Sea. *Palaeogeography, Palaeoclimatology, Palaeoecology* 292, 306–318.
- Wilson, G.S., Harwood, D.M., Askin, R.A., Levy, R.H., 1998. Late Neogene Sirius Group strata in Reedy Valley, Antarctica: a multiple-resolution record of climate, ice-sheet and sea-level events. *Journal of Glaciology* 44, 437–447.
- Zachos, J., Pagani, M., Sloan, L., Thomas, E., Billups, K., 2001a. Trends, rhythms, and aberrations in global climate 65 Ma to present. *Science* 292, 686–693.
- Zachos, J.C., Shackleton, N.J., Revenaugh, J.S., Pälike, H., Flower, B.P., 2001b. Climate response to orbital forcing across the Oligocene–Miocene boundary. *Science* 292, 274–278.
- Zinsmeister, W.J., de Vries, T.J., 1983. Quaternary glacial marine deposits on Seymour Island. *Antarctic Journal of the United States* 18, 64–65.